Generation of Gene Targeted Knockout Pig Fetuses and Evaluation of Off-Target Activity

By

KELLY ANNE ZACANTI
DISSERTATION

Submitted in partial satisfaction of the requirements for the degree of

DOCTOR OF PHILOSOPHY

in

Animal Biology

in the

OFFICE OF GRADUATE STUDIES

of the

UNIVERSITY OF CALIFORNIA

DAVIS

Approved:

Trish Berger, Chair

Elizabeth Maga

James Murray

Committee in Charge

2022

Table of Contents

Acknowledgements

I would like to acknowledge everyone that has supported me throughout my PhD. I would not be where I am today without the support of my major professor, Dr. Trish Berger. She wholeheartedly supported my academics, research, and career goals. She pushed me outside of my comfort zone, allowing me to grow as a scientist and critical thinker. Her optimism pushed me to continue after failed experiments, while her guidance supported my next steps to finding a solution. I am truly grateful to have had Trish as my major professor. I would also like to thank my committee members Dr. Elizabeth Maga and Dr. Jim Murray. They both provided support during my qualifying exam, one of the most challenging hurdles during my PhD, as well as support and mentorship for my research. Dr. Pablo Ross and the Ross lab also made this research possible. I would like to thank Pablo for his help and expertise on CRISPR/Cas9 and embryo production and the Ross Lab for providing a space for me to work and learn. Embryo transfers would not have been possible without veterinarians Dr. Brett McNabb, Dr. Joan Rowe, and their supporting students. I would also like to thank Aaron Prinz and all employees at the UC Davis Swine Facility for their help with the care and maintenance of the pigs, as well as during embryo transfers.

The Berger lab would not have been the same without Barbara Jean Nitta-Ota. I am forever grateful for her honesty and encouragement. She not only supported me with my research but also as a mentor and friend. I would like to give a special thanks to Insung Park. We worked together for years collecting oocytes, producing pig embryos, and during embryo transfers. I am grateful for the support he provided working with CRISPR/Cas9 and embryo production, as well as his friendship.

Most importantly, I would like to thank my friends and family. I am grateful for this experience because I met two of my closest friends, Erika Paulson and Tawny Scanlan. I wouldn't have made it through the years without their encouragement, friendship, and support. My aunt and uncle, Susie and Remy Cordier provided a home away from home in Davis. They provided me with endless love, support, game nights, and Sunday night dinners. I am grateful for the love, support, and patience Brandon Gundayao has given me over the years. His positivity and words of encouragement pushed me to continue every day. Lastly, I would like to thank my family. My mom, Dena Zacanti, provided words of encouragement, advice, and love every step of the way. She is my biggest supporter and inspires me every day. Thank you to my sister Becca Zacanti, grandma Esther Herrington, and dad Jim Zacanti for believing in me when I felt discouraged and motivating me to do my best. Although some of the most challenging years of my life, I am grateful to have had support from my major professor, my professors, and my friends and family.

Abstract

The use of genome engineering to manipulate biological systems and organisms has enabled a broad range of research for applications in basic science, medicine, biotechnology, and agriculture. The following research used CRISPR/Cas9 technology to generate pigs with nonfunctional genes of interest.

Clustered regularly interspaced palindromic repeats (CRISPR)/Cas9 is an efficient, RNA-guided endonuclease technology that specifically targets and mutates a selected gene of interest. Androgen receptor (AR) is a gene of interest targeted for mutation in this research. Androgens are steroid hormones that regulate the development and maintenance of the male reproductive system via androgen receptors. This research aims to create AR knockout pigs to render male pigs sterile and be a novel approach to genetic containment, a major concern of genetically modified animals. Although containment looks different depending on the species, effective containment strategies are necessary to ensure modified genes are not introduced into free-ranging animals.

When using CRISPR/Cas9 technology for genome engineering, off-target mutations are a challenge. Off-target activity could lead to mutations at unintended sites, potentially resulting in loss of gene function and unintended phenotypes. High frequency of off-target activity for RNA-guided endonuclease (RGEN)-induced mutations has been reported; however, reported off-target detection used in silico and in vitro methods, which cannot precisely predict mutations that occur in vivo. This research aims to generate steroid 5 alpha reductase 2 (SRD5A2) and JUNO knockout pigs to evaluate gRNA/Cas9 off-target activity in two unrelated genes of interest, as well as further understand the mechanism behind boar taint and the mechanism behind mammalian fertilization. SRD5A2 is the enzyme that synthesizes a compound responsible for

boar taint, a stale urine and fecal odor and flavor in meat from boars. Animal welfare concerns surrounding castration, the current method to remove boar taint, are the driving force to develop practical methods to eliminate boar taint. Juno, an oocyte plasma membrane protein, and Izumo1, a sperm cell surface protein, have been identified as the first cell-surface receptor pair essential for fertilization in the mouse. While Juno has been shown to be conserved across multiple species, conservation of its function has not been confirmed.

For each gene of interest, guide RNAs (gRNAs) were designed and tested for mutation efficiency in pig blastocysts. Once confirmed as efficient, gRNA or a combination of gRNAs and Cas9 protein were introduced into in vitro fertilized (IVF) zygotes via electroporation. Electroporated embryos were then transferred via embryo transfer into recipient sows. Twenty-two- to 24-day old knockout fetuses were collected for all three genes of interest, demonstrating fetal viability to 24 days. For the AR locus, guide RNAs targeting exon 2 and exon 5 were compared. Although proportion of conceptuses collected as fetuses did not differ for conceptuses with edits at exon 2 compared with edits at exon 5 in co-transfer experiments, survival tended to be higher for conceptuses with edits at exon 2 ($P=0.07$). All AR knockout fetuses obtained, were determined to be female (XX), which was significantly different from an expected 50:50 ratio ($P<0.001$). Blastocyst sexing was also evaluated for AR knockouts, showing no significant difference when compared to wild type (WT) frequencies. For SRD5A2 and JUNO 22- to 24-day knockout fetuses, potential off-target sites were identified for each gRNA and evaluated via Sanger sequencing for off-target activity. All potential off-target sites demonstrated no off-target activity in both knockout fetuses and knockout blastocysts.

These studies demonstrated fetal viability to 24 days for conceptuses with edits to three genes of interest. The gRNAs used to target two genes of interest also demonstrated no off-target activity at multiple predicted off-target sites.

Chapter 1: Literature Review

1.1 Introduction

The ability to make targeted modifications in a genome to manipulate biological systems and organisms opens the door for applications in basic science, medicine, biotechnology, and agriculture. Genome engineering refers to targeted modifications to alter an organism's genetic code; including its contexts (epigenetic level) or its outputs (transcripts) (Hsu et al., 2014). It can be used for applications in drug development, gene surgery, animal models of disease, genetic variation, fuel, food, and materials (Hsu et al., 2014).

The first transgenic mammals were generated in 1980. Gordon et al. successfully transferred a recombinant plasmid containing viral DNA via microinjection into the pronuclei of fertilized mouse embryos (Gordon et al., 1980). After implantation and development to full term, 2 of 78 newborn mice showed homology (although rearranged) to the injected plasmid DNA, demonstrating the first gene introduction into the murine genome (Gordon et al., 1980). Shortly after, in 1981, transgenic mice containing the rabbit ß-globin gene were generated and demonstrated transmission of the rabbit ß-globin gene to a fraction of their progeny (Costantini and Lacy). In 1982, transgenic mice that produced rat growth hormone (GH) were the first to demonstrate a change in phenotype produced from genetic engineering (Palmiter et al., 1982). The first genetically engineered livestock were generated in 1985 by microinjection of a metallothionein -growth hormone fusion gene into the pronuclei or nuclei of eggs from superovulated rabbits, sheep, and pigs (Hammer et al., 1985). All three species integrated the gene and expression was seen in transgenic rabbits and pigs. In the last 40 years, numerous genetically engineered organisms have been generated and the technology to create them has evolved. Modern genetic engineering techniques utilize nucleases to induce targeted mutations

whereby nucleases are guided to a specific target sequence within the genome to create a double strand break (DSB) in the DNA. The DSBs are then repaired by endogenous DNA repair pathways resulting in genetic modification. These techniques thus take advantage of a cell's DNA repair mechanisms to modify the genome.

1.2 Double Strand Break Repair Pathways

There are multiple causes of DNA DSBs in cells. DSBs are caused in normal development during meiosis by Spo11, a topoisomerase II-like enzyme (Zickler and Kleckner, 1999). During prophase I of meiosis, Spo11 creates DSBs which induce crossing over between homologues. These events are resolved by homologous recombination (Lieber, 2010). Harmful breaks also occur from reactive oxygen species (ROS), natural ionizing radiation in the environment, intracellular action by nuclear enzymes on DNA, and physical or mechanical stress on the DNA duplex (Lieber, 2010). During normal oxidative respiration, mitochondria convert oxygen to superoxide (O^{-}_{2}). Enzymes in the mitochondria can convert superoxide to hydroxyl free radicals, which react with DNA and cause single strand breaks (SSBs). Two closely spaced SSBs on anti-parallel strands will cause DSBs (Chance et al., 1979). Natural ionizing radiation from the environment, gamma and X-rays, create free radicals when they pass through organisms. When clusters of free radicals come close to DNA, they generate DSBs and SSBs (Lieber, 2010). Inadvertent action by nuclear enzymes include failures of type II topoisomerases, breaking both strands of DNA. If the topoisomerase fails to rejoin the strands, a DSB occurs (Adachi et al., 2003). Lastly, physical or mechanical stress on the DNA can cause DSBs. Telomere failures can result in chromosomal fusions, resulting in physical stress on the mitotic spindle with DSBs (Bailey and Murnane, 2006). No matter the cause, if unrepaired, DNA DSBs in a cell will cause cell death.

DSBs trigger DNA repair by one of two mechanisms, nonhomologous end joining (NHEJ) or homology-directed repair (HDR). NHEJ is an error-prone pathway that involves direct ligation of the cleaved ends back together with no sequence homology required. The direct ligation can cause insertions and/or deletions (indels) of varying sizes at the DSB site, resulting in mutations such as in-frame amino acid deletions or insertions, or frameshift mutations. For genome engineering, these mutations would ideally lead to disruption of the open reading frame (ORF), resulting in premature stop codons and gene disruption (Bibikova et al., 2002).

In NHEJ in eukaryotes, the Ku70-Ku80 heterodimer (Ku) recognizes DSBs in DNA and acts as a loading protein to recruit other NHEJ proteins needed to join the DNA ends. Once bound to DNA, Ku recruits DNA-dependent protein kinase catalytic subunit (DNA-PKcs), forming the DNA-PK complex (Meek et al., 2008). Ku also recruits DNA ligase IV and X-ray repair cross-complementing protein 4 (XRCC4). Both are the central components of NHEJ in eukaryotes. XRCC4-like factor (XLF), which has structural similarity to XRCC4, interacts with XRCC4 and forms a sleeve-like structure around DNA (Ahnesorg et al., 2006; Brouwer et al., 2016). It is presumed that the sleeve stabilizes the ends before covalent ligation, but the role of this structure is still not fully understood (Brouwer et al., 2016). Recruitment of these proteins can occur in any order, providing flexibility to the process. As most DSBs result in incompatible DNA ends, processing needs to occur prior to ligation. Nuclease activity known as resection is needed to ensure the ends are compatible. Resection involves the degradation of short regions of the 5’ or 3’ overhangs by nuclease activity to facilitate end joining. DNA-PKcs is recruited with the endonuclease Artemis. Artemis is activated and gains the ability to cleave single-stranded DNA overhangs (Gu et al., 2010; Chang and Lieber, 2016). While other nucleases may contribute to DSB repair, the Artemis-DNA-PKcs complex appears to be the primary nuclease

(Chang et al., 2015). For NHEJ, the array of diverse DNA substrates that can be used during ligation allows for mechanistic flexibility and a diversity of outcomes. Processing factors, including polymerases, nucleases, and structure-specific end cleaning enzymes are typically the point where mutations are introduced in the DNA sequence.

Homology directed repair is a significantly less predominant repair pathway that requires the presence of homologous DNA sequences, which are used as templates to repair DSBs in the DNA. By introducing donor DNA template with homology sequence flanking the DSB, researchers can take advantage of the HDR pathway to create a point mutation or insert a desired sequence. While the NHEJ pathway is highly prevalent and efficient, mutations are random. The HDR repair pathway is less common and efficient but can create precise mutations and specific insertions (Sander and Joung, 2014; Harrison et al., 2014). For HDR, the 5'-end DNA strand undergoes resection at the break to create a 3' overhang, serving as a substrate for proteins required for DNA strand invasion by Rad51, or a related recombinase, and a primer for DNA repair synthesis (Sung et al., 2003). The invasive strand displaces one strand of the homologous DNA duplex and pairs with the other, resulting in the formation of the hybrid DNA referred to as the displacement loop (D loop). Recombination intermediates are then resolved to complete DNA repair (Pardo et al., 2009). For use in genetic engineering, HDR factors can be used to promote HDR over NHEJ after a DSB to aid in a successful knock-in. This process has been demonstrated in human cell lines such as HEK293T and embryonic stem cells (Nambiar et al., 2019; Rees et al., 2019). Alternatively, reducing NHEJ proteins Ku70 and Xrcc4 is an approach to enable HDR (Bertolini et al., 2009). It was demonstrated in human HCT116 cells that a transient knockdown of Ku70 and Xrcc4 via RNAi treatment led to a 70% reduction in random integration events and a 33-fold increase in the efficiency of gene targeting (Bertolini et al.,

2009). Inhibitors against the cell cycle regulator of NHEJ (CYREN) have also been studied (Arnoult et al., 2017), as well as a Cas9 fusion to dominant-negative 53BP1 plasmid to enhance HDR and inhibit NHEJ at Cas9 cut sites (Jayavaradhan et al., 2019). Different approaches to promote HDR over NHEJ may be used depending on numerous factors including the methods used, cell type, and the gene or genes of interest. Both DNA repair pathways can be utilized to modify the genome, leading to a variety of applications.

1.3 Utilizing DNA Repair for Genome Engineering

Modern genetic engineering technologies utilize engineered nucleases or a RNA-guided system to create DSBs in the DNA, which then stimulates a DNA repair pathway resulting in modification at specific sites of interest. Zinc-finger nucleases (ZFNs) are fusion proteins comprised of DNA binding C_2H_2 zinc fingers fused to the nonspecific DNA cleavage domain of the nuclease Fok1 (Harrison et al., 2014). Fok1cleavage domains must dimerize to be active, so two ZFNs are required to create DSBs. Individual zinc fingers are engineered to recognize a nucleotide triplicate. Specific genome sequences are targeted by joining together multiple zinc fingers. To create DSBs, ZFNs are designed in pairs to recognize sequences on the forward and reverse strands. Once ZFNs bind, Fok1 domains dimerize and cleave the DNA creating a DSB, which leads to cellular repair via NHEJ or HDR (Urvov et al., 2010). Due to the nature of ZFNs, it can be challenging technology to work with. Protein engineering is difficult and site selection is limited (Gupta and Musunuru, 2014). Limited site selection restricts the potential target sites. Off-target activity is also a significant concern. Two studies looking at off-target activity with the use of ZFNs found off-target activity at multiple loci in cultured human tumor cells (Gabriel et al., 2011; Pattanayak et al., 2011).

Similar to ZFNs, transcription activator-like effector nucleases (TALENs) utilize Fok1 dimerization to create DNA DSBs for genome engineering. TALENs are proteins comprised of a Fok1 nuclease fused to a DNA binding domain, which is composed of TAL effectors (TALEs), proteins secreted by Xannthomonas spp. bacteria to alter gene transcription in host plant cells (Boch and Bonas, 2010). TALEs have a central DNA binding region comprised of a tandem array of nearly identical repeats. Residue 13 in the array specifies the identity of a single nucleotide (Mak et al., 2013). Thus, this protein-DNA code is used as a tool to identify which TALEs to use to target a specific base and fusion of an array of TALEs can be used to target a specific DNA sequence. Like ZFN, two TALENs are composed either side of the desired DSB and each fused to FokI so when DNA binding occurs, the FokI is dimerized and can induce a DSB. Compared to ZFNs, TALENs are easier to construct using this direct protein-DNA code and are engineered to recognize 30 to 40 base pair targets. Engineering TALENs using proteins that correspond with individual nucleotides makes TALENs easier to design than ZFNs with fewer limits on site selection. However, protein engineering remains a difficult task. Similar to gene disruption activity using ZFNs, TALENs also induces off-target activity (Mussolino et al., 2011). Off-target activity using TALENs can be reduced by choosing unique target sequences that differ by at least 7 nucleotides from any other site in the genome (Kim et al., 2013; Koo et al., 2015). In 2013, an RNA-guided technology simplified genetic engineering.

Clustered regularly interspaced palindromic repeats (CRISPR)/CRISPR-associated protein 9 (Cas9) has become a popular genetic engineering tool for biological and biomedical research due to its simplicity and efficiency compared to TALENs and ZFNs. Clustered regularly interspaced palindromic repeats (CRISPRs) were first described after observation of a series of short direct repeats interspaced with short sequences in the *E. coli* genome (Ishino et al., 1987).

They were later detected in numerous bacteria and archaea (Mojica et al., 2000). The pivotal finding that many of the observed spacer sequences were derived from plasmid and viral origins led to the notion that CRISPR/Cas is an adaptive defense mechanism against viral predation and foreign nucleic acids in bacteria and archaea (Bolotin et al., 2005; Mojica et al., 2005; Pourcel et al., 2005). The first experimental evidence of CRISPR/Cas as an adaptive immune response in bacteria was in 2007 using lactic acid bacterium with lytic phages (Barrangou et al., 2007). Nine phage-resistant *Streptococcus thermophilus* mutants were generated by challenging the wild type (WT) strain with two different phages. Their CRISPR loci were analyzed, showing 1 to 4 additional spacers inserted next to the spacers present in the WT strain. These results demonstrated the CRISPR was modified by the integration of new spacer sequences, retaining infection information from phage DNA. This led to the first successful application of CRISPR/Cas for biotechnology, as naturally occurring CRISPR/Cas systems in cultured bacteria could be used for immunization against phages in the dairy industry (Barrangou and Horvath, 2012).

In the CRISPR/Cas system, short sequences, referred to as protospacers, from a viral genome are copied as “spacers” between repetitive sequences in the CRISPR locus of the host genome (Sorek et al., 2013). The CRISPR locus is transcribed and processed into short CRISPR RNAs (crRNAs) that guide Cas, an endonuclease, to the complementary genomic target sequence. Cas nucleases require a PAM (protospacer adjacent motif) sequence 2 to 6 nucleotides downstream from the target DNA sequence in order for the Cas to cleave the DNA. Cleavage occurs approximately 3 to 4 nucleotides upstream of the PAM sequence.

CRISPR/Cas systems have been developed into RNA-guided endonucleases (RGENs) used to edit genomes (Horvath and Barrangou, 2010). There are three CRISPR/Cas system types:

type I, type II, and type III. Each type uses a distinct mechanism to recognize and cleave nucleic acids. Type I and type III use a large complex of Cas proteins for RNA-guided targeting, while the type II system requires only a single protein for RNA-guided DNA recognition and cleavage (Doudna and Charpentier, 2014). Of the three systems, type II has been adapted to be used as a genetic engineering tool and is effective to genetically engineer mammalian cells. The type II CRISPR system utilizes a guide RNA (gRNA) and an endonuclease, typically Cas9 (CRISPR-associate protein 9, from *Streptococcus pyogenes*), to create a DNA DSB at the targeted genome locus (Jinek et al., 2012). Cas9 is the most commonly used Cas protein, which requires a PAM sequence of 5'-NGG-3' to cleave the target DNA. Alternative sequences can be targeted using other Cas9 orthologs, which have different PAM sequences (Hsu et al., 2014). In this system, crRNA binds with tracrRNA (trans-acting CRISPR RNA) to recruit the Cas9 nuclease to the DNA target sequence (Deltcheva et al., 2011; Jinek et al., 2012). The system was simplified for use in the laboratory by fusing together a crRNA, tracrRNA, and a short (~20 nucleotide) RNA sequence to create a single chimeric gRNA (Gasiunas et al., 2012; Jinek et al., 2012). Although some early experiments showed a gRNA may not be as efficient as introducing a crRNA and tracrRNA, the ease of using a single gRNA has led to their widespread use for genome engineering (Mali et al., 2013b).

Once introduced into a cell, Cas9 is recruited by either a crRNA-tracrRNA pair or a chimeric gRNA, both of which contain a ~20 nucleotide sequence that matches a target site of interest (Cho et al., 2013; Cong et al., 2013; Jinek et al., 2013; Mali et al., 2013b). The DNA target site must have a PAM sequence downstream in order for the Cas9 to recognize and cleave the target sequence. Heterologous expression of crRNA-tracrRNA complexes and gRNAs direct Cas9 to create a DSB within the genome and induce NHEJ or HDR (Cong et al., 2013;

Deltcheva et al., 2011; Mali et al., 2013b). The nature of this system also allows for targeting of several genes at once.

Cas9 proteins contain two trademark nuclease domains: RuvC and HNH. The crystal structure of *Streptococcus pyogenes* Cas9 has been reported and shows a bilobed architecture including a target recognition lobe and a nuclease lobe, which accommodates a gRNA:DNA heteroduplex in a groove (Jinek et al., 2014; Nishimasu et al., 2014). The recognition lobe is responsible for binding gRNA and DNA, while the nuclease lobe, which contains the HNH and RuvC nuclease domains, cleaves the complementary and noncomplementary strands of the target DNA. The nuclease lobe also contains a domain responsible for interaction with the PAM sequence, which is necessary for Cas9 to bind with and cleave the target DNA (Nishimasu et al., 2014). Once the gRNA is bound to Cas9, Cas9 undergoes a conformational change, turning the inactive, non-DNA binding conformation to an active DNA-binding conformation. The spacer sequence of the gRNA remains open to interact with target DNA, while the Cas9/gRNA complex binds near a PAM sequence. Cas9 will cleave the DNA when the spacer sequence matches its target (Jinek et al., 2014; Nishimasu et al., 2014).

Different approaches have been used to deliver gRNA and Cas9 into cultured mammalian cells including microinjection, electroporation, nucleofection, and lipofectamine-mediated transfection (Mali et al., 2013a; Fu et al., 2014). Lentiviral vectors also have been used to express Cas9 or gRNAs in cultured human and mouse cells (Shalem et al., 2014; Koike-Yusa et al., 2014). When using CRISPR/Cas9 to generate knockout or knock-in animals, microinjection and electroporation are preferred methods when working with embryos. Microinjection of in vitro-transcribed (IVT) Cas9 mRNA/plasmid DNA and gRNA/plasmid DNA has been used in one-cell embryos of zebrafish, mice, rats, fruit flies, pigs, cattle, sheep, and monkeys (Sander and

Joung, 2014; Bevacqua et al., 2016; Vilarino et al., 2017). The microinjection of gRNA and Cas9 into the pronucleus of one-cell mouse and zebrafish embryos resulted in the generation of genetically engineered organisms, specifically knockouts (Sung et al., 2014). About 90% of injected embryos developed into blastocysts and hatched, suggesting RNA guided endonucleases (RGENs) were not cytotoxic while maintaining high mutation frequencies (Sung et al., 2014). Recently, electroporation has been used successfully to introduce Cas9 protein and gRNA into pig zygotes to mutate a target gene of interest, generating genetically modified pigs after embryo transfer of electroporated, in vitro fertilized zygotes (Tanihara et al., 2020). Electroporation conditions vary by species and methods continue to be developed for use with CRISPR/Cas9 technology.

1.4 CRISPR/Cas9 Application and Challenges

CRISPR/Cas9's ability to create frameshift knockout mutations and sequence insertions leads to an array of applications including disease models, identification of gene function, correction of defective genes for therapeutic applications, and modification of genes to benefit the health and production of agricultural species (Reviewed in Garas et al., 2015 and Zhao et al., 2019). With the ability to disrupt multiple targets simultaneously, this technology can be used to study adjacent genes or create large fragment deletions. The construction of CRISPR libraries can also be used for genome-wide screening (Shalem et al., 2014; Koike-Yusa et al., 2014).

As with other genetic engineering systems, off-target mutations are a concern when using CRISPR/Cas9 technology. Off-target effects could cause mutations at unintended sites, potentially leading to loss of gene function and unintended and undesirable phenotypes (Naeem et al., 2020). Paired nickases, truncated gRNAs, and chemical modification of gRNA are some of the methods that can be used to mitigate off-target effects. Overall design of a specific and

efficient gRNA with low off-target effects is a mitigation strategy of its own. GC content between 40-60% in the gRNA sequence increases on-target activity, as higher GC content stabilizes DNA:RNA duplex and destabilizes off-target binding (Wang et al., 2014). Shortening the gRNA (truncated gRNA) length from 20 base pairs to 17 or 18 base pairs has been reported to reduce off-target events by 500-fold without affecting target accuracy (Fu et al., 2014). In addition, using truncated gRNAs with paired nickases can further reduce off-target effects in mammals (Ran et al., 2013; Fu et al., 2014). Cas9 nickase (Cas9n) is the mutated form of SpCas9 generated through the mutation of the HNH or RuvC domain. To utilize Cas9 nickase for genetic engineering, a pair of gRNAs are required to make an efficient DSB. The mutation renders Cas9 able to cleave only one strand complementary to the gRNA, thus requiring a pair to create a DNA DSB (Ran et al., 2013). Several methods of chemical modification of gRNA are also used to limit off-target activity. Incorporating 2'-O-methyl-3'-phosphonoacetate in the gRNA ribose-phosphate backbone causes a 40-120 fold decrease in off-target cleavage while still maintaining on-target activity (Ryan et al., 2018). CRISPR/Cas9 systems have even been developed to co-express gRNA that targets Cas9 encoded in viral vectors. This restricts the duration of expression of CRISPR/Cas9, overall reducing off-target effects (Chen et al., 2016). Researchers are working to develop engineered Cas9 variants with minor off-target effects to improve our current technologies.

A significant challenge to using CRISPR/Cas9 technology for genome engineering in embryos is the possibility of mosaicism in founder animals. Genetic mosaicism is the presence of two or more genotypes in an individual (Mehravar et al., 2019). Using the CRISPR/Cas9 system to generate knockout and transgenic animals, zygotes are microinjected simultaneously with the gRNA and either Cas9 RNA or Cas9 protein. This allows for the gRNA/Cas9 complex to

continuously target and cleave the target sequence at different stages of embryonic development, leading to mosaicism (Oliver et al., 2015; Yen et al., 2014). Mosaicism is undesirable for most CRISPR/Cas9 applications, as it can generate false-positive genotyping results and complicate both genotype and phenotype analysis in founder animals. Analyzing the offspring after breeding is a method that could be used to avoid genotyping and phenotyping errors of the founding animals; however, this process is not suitable for livestock species, as generating F1 and F2 generations could take years (Mehravar et al., 2019).

Understanding the mechanism behind CRISPR/Cas9 mediated genetic mosaicism may help minimize occurrences in genetically engineered organisms. Timing of cell division and DNA replication when using CRISPR/Cas9 plays a major role in resulting genetic mosaicism. If DNA cleavage from Cas9 endonucleases occurs at different stages during embryogenesis, gRNA/Cas9 complexes will still be active in daughter cells and mosaicism will occur. Additionally, it takes 15 hours for degradation of expressed Cas9 protein, making it more difficult to avoid mosaicism (Markossian and Flamant, 2016). If expression and activity of Cas9 is prolonged beyond the one-cell stage, mosaicism is anticipated (Jao et al., 2013; Yen et al., 2014). Additionally, due to the nature of NHEJ-mediated repair, the introduction of indels of random length will also play a role in contributing to genetic mosaicism. High frequencies of non-mutagenic repair from NHEJ may result in undesirable mosaicism, as mutagenic repair at the target site competes with cell division rates (Hsu et al., 2014). When trying to create organisms with altered sequences or transgene insertions, individual cells can repair the DSB via NHEJ or HDR (Harrison et al., 2014). Repair events may be random indels or the predicted base changes at targeted insertions, leading to undesirable mosaicism. The target sequence, which can influence the base pair deletion size during NHEJ, and species, which influences different

mechanisms during genome engineering, can impact the likelihood of mosaicism (van Overbeek et al., 2016; Raveux et al., 2017). Lastly, the concentration of gRNA/Cas9 and their activity level may influence mosaicism.

Some strategies have been used to reduce mosaicism using the CRISPR/Cas9 system. Using IVT gRNAs and Cas9 mRNA rather than CRISPR/Cas9 plasmids and introducing Cas9 protein rather than Cas9 mRNA have decreased the occurrence of mosaicism in mice and zebrafish (Aida et al., 2015; Burger et al., 2016; Sung et al., 2014). The timing of introduction of CRISPR/Cas9 components has also been studied. Changing the time of microinjection in bovine embryos has shown significantly reduced mosaicism rates when CRISPR/Cas9 substrates were delivered sooner than the conventional 20 hours post insemination (hpi) (Lamas-Toranzo et al., 2019). Early zygote microinjection (10 hpi) or oocyte microinjection before fertilization significantly reduced mosaicism (~10-30% mosaic vs. the conventional 20 hpi rate of 100%). Another method used to limit mosaicism is to modify the germline indirectly using somatic cell nuclear transfer (SCNT). This method uses genetically modified somatic cells as nuclear donors into enucleated germ cells. SCNT of CRISPR/Cas9 edited cells has been used in pigs and goats to reduce mosaicism (Ni et al., 2014). Depending on the species, cell type, and target sequence, multiple tactics may be required to combat mosaicism. There are no absolute methods for elimination of mosaicism.

CRISPR/Cas9 technology has been developed to generate DNA DSBs within a cell and utilize its DNA repair mechanisms to alter the genome in a targeted manner. The technology serves as a powerful tool to genetically modify cells and organisms to advance basic science, biotechnology, medicine, and agriculture. Future research to refine the current systems could

reduce off-target activity and prevalence of mosaicism, further improving the technology and allowing for more precise genome editing.

1.5 Genes of Interest

Advancements in genome editing technologies have made generating genetically engineered animals easier and more accessible. Scientists can more easily manipulate genes of interest and create knockout or knock-in animal models to study basic science and agriculture. Three genes of interest include androgen receptor (AR), steroid 5 alpha reductase 2 (SRD5A2), and JUNO (folate receptor 4, FOLR4).

Both AR and SRD5A2 are significant to addressing boar taint, a stale urine and fecal odor and flavor in meat from boars. The current method to remove boar taint is castration. Animal welfare concerns surrounding castration have led a push to find alternatives to the current method. AR and SRD5A2 are involved in the mechanisms behind the primary components of boar taint. The two primary components of boar taint, androstenone and skatole accumulate in a boar's fat, leading to boar taint (Patterson, 1968; Robic et al., 2008). Androgen production in the testis is associated with increased androstenone levels, therefore making AR a gene of interest, while the enzyme SRD5A2 synthesizes androstenone from its precursor androstadienone (Robic et al., 2014). Androstenone is not only a major component to boar taint but also inhibits the metabolism of skatole (Perry et al., 1980; Squires and Lundström, 1997), directly and indirectly targeting the elimination of boar taint.

In addition to the significance of studying boar taint, AR may also be a potential novel approach to genetic containment as it has been demonstrated to render animals sterile (Yeh et al., 2002; De Gendt et al., 2004; De Gendt et al., 2005; Notini et al., 2005; Lim et al., 2009; Tsai et

al., 2006). Stacking an AR knockout with other gene edits would allow for terminal propagation of the desired trait in male offspring. SRD5A2 is not theorized to lead to sterility.

The mechanism behind mammalian fertilization is not fully understood. Juno and Izumo1 have been identified as the first cell-surface receptor pair essential for fertilization in the mouse (Bianchi et al., 2014). Izumo1 is a protein present under the acrosomal cap of sperm, whose receptor, Juno (folate receptor 4, Folr4) is a protein present on the oocyte plasma membrane. Although Juno and Izumo1 have been identified in multiple species other than the mouse including humans, pigs, and opossums, determining whether their function during fertilization is conserved across species has not been confirmed. Generating JUNO-knockout pigs to study gene function is key to further our understanding of the mechanism behind mammalian fertilization.

Gene-editing technologies can be used to study specific genes of interest like AR, SRD5A2, and JUNO. All three genes of interest are important to reproductive biology and animal production.

Chapter 2: Generation of Androgen Receptor Knockout Pig Fetuses via CRISPR/Cas9 Technology

2.1 Introduction

Genetic engineering has the potential to improve animal health, nutrition, and production; however, producers and the public have concerns regarding the use of these technologies in food animals. One major concern is the containment of genetically modified animals. Containment looks different depending on the species; however effective containment strategies are necessary to ensure modified genes are not introduced into wild-type animals. One method to ensure genetic containment among a population would be to render genetically modified animals infertile via gene editing.

Androgens are steroid hormones that regulate the development and maintenance of reproductive, cardiovascular, immune, neural, and hemopoietic systems via androgen receptors (ARs), ligand-dependent nuclear transcription factors and members of the steroid hormone nuclear receptor family (Davey and Grossmann, 2016; MacLean et al., 1997). Androgens testosterone and dihydrotestosterone (DHT) are male sex hormones that regulate the development and maintenance of the male reproductive system. Their actions are mediated via ARs (Davey and Grossmann, 2016). Androgen receptors are comprised of three functional domains: the N-terminal transcriptional regulation domain, the DNA binding domain, and the ligand binding domain (MacLean et al., 1997). Located on the X chromosome, the AR gene has nine exons in the pig, while the mouse and human genes have eight exons. In mice, modification of exons 1, 2 and 3 of the AR gene leads to various phenotypic outcomes including reduced testosterone, reduced 5-alpha reductase, smaller, cryptorchid testes, decreased Leydig cell number, reduced Sertoli cell number and capacity to support spermatogenesis, feminized genitalia, and incomplete, arrested spermatogenesis (Yeh et al., 2002; De Gendt et al., 2004; De

Gendt et al., 2005; Notini et al., 2005; Lim et al., 2009; Tsai et al., 2006). The various effects on male reproductive phenotypes in mice suggest knocking out AR in pigs is also likely to hinder male reproduction. Due to its location on the X chromosome, knocking out AR in pigs would be a novel approach to genetic containment as it would render male pigs sterile. Founder males, all male offspring from founder females, and half of male offspring from heterozygous F1 females will lack a functional AR and be infertile. When stacked with other gene edits, this approach would allow for terminal propagation of the desired trait in male offspring.

Nonfunctional AR also has the potential to eliminate a substrate that causes boar taint, a stale urine and fecal odor and flavor in meat from boars. As pressure builds to find alternatives to castration, finding a dependable alternative that guarantees complete elimination of boar taint is imperative (Valeeva et al., 2009). Boar taint is primarily caused by the accumulation of androstenone and skatole in a male pig's fat (Patterson, 1968; Robic et al., 2008). Androstenone is an androgen metabolite that is produced in the testis, while skatole is a tryptophan metabolite produced by bacterial degradation in the hind gut (Perry et al., 1980; Squires and Lundström, 1997). Androstenone also inhibits the metabolism of skatole, making it an ideal target for the elimination of boar taint. In addition to genetic containment, knocking out AR in male pigs has the potential to decrease androgens in the testis, preventing the formation of androstenone, a knockout that directly and indirectly targets the elimination of boar taint.

Generating AR knockout pigs is conceivably an effective biocontainment method for genetically engineered animals, as well as a potential method to eliminate boar taint without the need for castration. CRISPR/Cas9 technology was used in this study to target and mutate specific loci within the pig AR gene to generate knockout fetuses. gRNAs were designed and tested for efficiency at generating indels (insertions or deletions) in pig embryos. Efficient gRNAs and

Cas9 protein were then introduced into pig embryos via electroporation before transfer into recipient sows. Fetuses were harvested and analyzed for mutations at the target loci. Additionally, RNA expression of AR was assessed in wild type fetuses.

2.2 Materials and Methods

2.2.1 Animal Care

All experiments were approved and performed in accordance with the Institutional Animal Care and Use Committee (IACUC) at the University of California, Davis. All animals were housed at the UC Davis Swine Facility.

2.2.2 Guide RNA and Primer Design

Guide RNAs (gRNAs) were designed using a CRISPR design tool from the Zheng laboratory at MIT (crispr.mit.edu) to target exons 2 and 5 of the AR gene in the *Sus Scrofa* genome. Three gRNAs were identified from the CRISPR design tool results and selected to avoid off-target events. CRISPRevolution sgRNA EZ Kits (Synthego, Menlo Park, CA) were purchased for each selected gRNA to test for gene editing efficiency in blastocysts. Primers were designed using the National Center for Biotechnology Information's primer design software, NCBI's Primer-BLAST (Ye et al., 2012), to amplify regions of the AR gene containing each gRNA target site. Amplicons ranged from 610 to 1170 base pairs in size to detect mutations surrounding each target site.

2.2.3 Embryo Production

2.2.3a Oocyte Collection and Maturation

Pig ovaries were collected from a slaughterhouse (Olson Meat Company, Orland, CA) and transported to the laboratory in a thermos with saline (35°C). Oocytes were aspirated from medium sized follicles (3-5 mm) with a 20-guage needle attached to a 10 ml syringe. Collected

follicular fluid was transferred to a Petri dish and searched for oocytes. Oocytes were washed in IVM1 maturation medium (TCM-199 (Gibco M2154) supplemented with 20% porcine follicular fluid, 50 μg/mL gentamicin, 100 μg/mL cysteine, 0.91 mM sodium pyruvate, 3.05mM D-glucose, 0.5 mg/mL FSH, 0.5 mg/mL LH, and 100 ng/mL EGF) and placed in a final drop of IVM1 covered in mineral oil and placed in an incubator (38.5°C, 5% CO_2, 5% O_2, approximately 90% humidity) for 20 to 24 hours. Oocytes were then moved into a new plate containing IVM2 maturation medium (TCM-199 (Gibco M2154) supplemented with 20% porcine follicular fluid, 50 μg/mL gentamicin, 100 μg/mL cysteine, 0.91 mM sodium pyruvate, 3.05mM D-glucose, and 1 mM cAMP) for an additional 20 to 24 hours of maturation. Oocytes were matured for a total of 40 to 44 hours to the M2 stage.

2.2.3b In Vitro Fertilization

Once matured to the M2 stage, oocytes were stripped of their cumulus cells using hyaluronidase (1 mg/ml) and washed in Tris-Buffered Medium (TBM) (sterile ultrapure water containing 113.1 mM NaCl, 3 mM KCl, 7.5 mM $CaCl_2 \bullet 2H_20$, 20 mM Tris Base, 11 mM D-glucose, 5 mM sodium pyruvate, 2 mg/mL bovine serum albumin, 1mM caffeine, pH 7.3-7.4 after equilibration, and phenol red). Five 90 ul drops of TBM medium were placed in each 60 mm Petri dish. Groups of 20 oocytes were pipetted into the 90 μl drops of TBM and plates were placed into an incubator (38.5°C, 5% CO_2, 5% O_2, approximately 90% humidity).

Fresh semen was collected from boars housed at the UC Davis Swine Facility and transferred to the laboratory in a light-protected 50 ml conical tube. In the laboratory, semen was kept warm on a heat block (38°C). Sperm motility was assessed by viewing a 5 μl drop of raw semen on a slide under a compound microscope. One hundred μl of semen was pipetted into a 15 ml conical tube containing 1.9 ml of TBM medium and the sperm were washed by centrifugation

(120 x g) for 3 minutes. Supernatant was aspirated and discarded and TBM (1.9 ml) was added to the sperm pellet and gently pipetted to mix. The sperm were washed again by centrifugation (100 x g for 3 minutes), supernatant was aspirated and discarded and TBM (500 µl) was added to resuspend the pellet. Sperm motility was then assessed, as previously stated and sperm were counted using a hemocytometer. Oocytes were fertilized by adding 10 µl of sperm prepared in TBM medium with the concentration adjusted to 1,000 sperm per oocyte (20,000 sperm per 10 µl). Oocytes were co-incubated with sperm for 5 to 6 hours. Presumptive zygotes were washed in PZM-5 medium (108 mmol NaCl, 25.07 mmol $NaHCO_3$, 10 mmol KCl, 0.35 mmol KH_2PO_4, 0.4 mmol $MgSO_4 \bullet 7H_2O$, 2 mmol Ca(lactate)$2 \bullet 5H_2O$, 0.2 mmol sodium pyruvate, 2 mmol L-glutamine, 5 mmol hypotaurine, 2% MEM Essential Amino Acids (50x), 1% MEM Non-Essential Amino Acids (100x), 0.05 mmol/L gentamicin, 3 mg/mL BSA), moved to a 4-well plate containing PZM-5 medium and incubated.

2.2.4 Guide RNA Evaluation in Embryos

2.2.4a Microinjection and Electroporation

Zygotes were microinjected with Cas9 mRNA and gRNA or combination of gRNAs via cytoplasmic microinjection. Any embryos that divided before microinjection were discarded. Zygotes were microinjected an estimated 9 to 10 hours post-fertilization. Guide RNAs were diluted to a final concentration of 25ng/µL. When a combination of gRNAs was microinjected into zygotes, their combined final concentration was also 25ng/µL. The concentration of the Cas9 mRNA was 50ng/µL. Approximately 6 to 8pL of gRNA/Cas9 were microinjected into each zygote.

Electroporation of pig embryos was performed using a NEPA21 Type II Super Electroporator (NEPAGENE, Ichikawa, Japan). Nine hours post-fertilization, 35 to 50 embryos

were moved into SOF-HEPES followed by washing through three drops of Opti-MEM™ (Gibco). Embryos were moved into a drop containing 10 µl Opti-MEM™, 5 µl Cas9 protein (200 ng/µl), and 5 µl gRNA (100 ng/µl) or combination of gRNAs (100 ng/µl). The 20 µl drop containing embryos was pipetted into a 1 mm gap cuvette (BioRad, Cat No. 1652083). Electroporation was performed using a poring pulse (5 x 1 ms pulses at 30V). After electroporation, embryos were moved to PZM-5 medium and incubated.

Compared to microinjection, electroporation is a simpler and more efficient technique that allows for larger numbers of embryos to be exposed to Cas9 and gRNA.

2.2.4b Embryo Collection and Sequencing

Genomic DNA from embryos was sequenced to detect CRISPR/Cas9 induced indels (insertions or deletions). Individual blastocysts were collected 6 days post-electroporation and placed into 0.2 ml PCR tubes containing 10 µl of lysis buffer (Epicentre). After vortex and centrifugation, tubes were incubated at 65°C for 6 minutes and 98°C for 2 minutes. Lysed embryos were stored at -20°C until PCR reaction. Two rounds of PCR were performed using GoTaq Green Master Mix (Promega Biosciences) and specific primers designed to flank each target AR sequence (Table 2.6.2). The first reaction used 9.2 µl of lysed embryo, while the second reaction used 5 µl of PCR product from the first reaction. The PCR conditions were 5 minutes at 95°C, followed by 35 cycles of 45 seconds at 95°C, 45 seconds at annealing temperature (Table 2.6.2), and 1 minute at 72°C. After 35 cycles, reactions concluded with 7 minutes at 72°C. PCR products were loaded onto a 0.8% agarose gel (1X TBE buffer) and separated by gel electrophoresis. Bands were excised under UV transillumination using a clean razor blade. DNA was extracted and purified using the QIAquick Gel Extraction Kit (Qiagen). Extracted DNA was submitted to Genewiz (South San Francisco, CA) for Sanger sequencing.

Sequences were aligned to the reference sequence using SnapGene® (from Insightful Science; available at snapgene.com) and CRISP-ID (Dehairs et al., 2016) software.

2.2.5 Embryo Transfers and Fetus Evaluation

2.2.5a Embryo Transfers

Estrus was induced in recipient gilts by injection of P.G. 600® (400 IU pregnant mare's serum gonadotropin and 200 IU human chorionic gonadotropin per dose, Merck, Kenilworth, NJ) followed by Chorulon® (750 IU human chorionic gonadotropin per dose, Merck). Estrus was monitored prior to embryo transfer.

One to two days after electroporation with Cas9 protein and gRNA or a combination of gRNAs, 2- to 4-cell embryos were selected for transfer. Embryos at the same stage of development were transferred into recipients. Recipient gilts were injected with Telazol® (Zoetis, Parsippany, NJ) for sedation and anesthetized using isoflurane administered by inhalation. Veterinarians performed a medial laparotomy for embryo transfer, delivering electroporated 2- to 4-cell embryos into both oviducts via a 0.5 ml straw attached to a 1 ml syringe. Equal numbers of gRNA/Cas9 electroporated embryos (total of 64-80 embryos) targeting exon 2 and exon 5 were typically transferred into each recipient with half of each target placed in each oviduct.

2.2.5b Fetus Collection and Analysis

Recipient gilts were slaughtered and fetuses were collected 22- to 24-days post-embryo transfer. Tail samples were removed and DNA was extracted using Qiagen's DNeasy Blood and Tissue Kit. DNA concentration was determined by nanodrop (Thermo Scientific NanoDrop™ 2000). Sex of each fetus was determined by performing PCR using GoTaq Green Master Mix (Promega Biosciences) and previously confirmed X and Y specific primers (Table 2.6.2) (Aasen

and Medrano, 1995; Pomp et al., 1990). PCR conditions were 5 minutes at 95°C, followed by 30 cycles of 30 seconds at 95°C, 30 seconds at 55°C, and 30 seconds at 72°C, concluded with 7 minutes at 72°C. PCR products were visualized on a 2% agarose gel (1X TBE buffer) with SYBR™ Safe DNA gel stain (Invitrogen™) using a ChemiDoc-ItTS2 Imager (Analytik Jena US, Upland, CA).

To determine whether or not the target sequence was mutated, a single round of PCR was performed using extracted fetus DNA, GoTaq Green Master Mix (Promega Biosciences), and specific primers designed to flank each target AR sequence (Table 2.6.2) using PCR conditions previously described (*2.2.4b Embryo Collection and Sequencing*). PCR products were separated by gel electrophoresis on a 0.8% agarose gel (1X TBE buffer). Bands were excised under UV transillumination using a clean razor blade. DNA was extracted and purified using Qiagen's QIAquick Gel Extraction Kit. DNA was submitted to for Sanger sequencing. Sequences were aligned to the reference sequence using SnapGene® and CRISP-ID software.

2.2.6 XY Sequencing of Genetically Engineered Blastocysts

Zygotes were generated via IVF and electroporated with individual gRNA or a combination of gRNAs, as previously described. Individual blastocysts were collected in 10 µl of lysis buffer (Epicentre). After vortex and centrifugation, tubes were incubated at 65°C for 6 minutes and 98°C for 2 minutes. Lysed embryos were stored at -20°C until PCR reaction. PCR reactions were performed to determine sequencing at the target loci, as well as to determine the sex of each blastocyst. For each blastocyst, 5 µl of lysate was used for the initial XY PCR reaction and 5 µl was used for the initial sequencing reaction.

To determine the sex of each blastocyst, nested PCR was performed using GoTaq Green Master Mix (Promega Biosciences) with primers designed to amplify regions of the X and Y

chromosome (Table 2.6.2). PCR product from the first reaction (5 µl) was used for the second reaction. XY PCR conditions were previously described (*2.2.5b Fetus Collection and Analysis*). PCR products were visualized on a 2% agarose gel (1X TBE buffer) with SYBR™ Safe DNA gel stain (Invitrogen™) using a ChemiDoc-ItTS2 Imager (Analytik Jena US, Upland, CA) to determine sex.

For sequencing of target sites, nested PCR was performed using GoTaq Green Master Mix (Promega Biosciences) with specific primers designed to amplify each target AR sequence (Table 2.6.2). The first reaction used 5 µl of lysate, while the second reaction used 5 µl of PCR product from the first reaction. PCR conditions were previously described (*2.2.4b Embryo Collection and Sequencing*). After the second PCR reaction, products were loaded onto a 0.8% agarose gel (1X TBE buffer) and separated by gel electrophoresis. Bands were excised under UV transillumination using a clean razor blade. DNA was extracted and purified using the QIAquick Gel Extraction Kit (Qiagen). Extracted DNA was submitted to Genewiz for Sanger sequencing. Sequences were aligned to the reference sequence using SnapGene® (from Insightful Science; available at snapgene.com) and CRISP-ID software (Dehairs et al., 2016).

2.2.7 RNA Expression of Androgen Receptor in 19-Day Fetuses

RNA expression of AR was examined in unedited 19-day pig fetuses. A female was artificially inseminated with boar semen. At 19 days post-insemination, the female was slaughtered, and her reproductive tract was harvested. All fetuses were collected and stored at -80°C. The sex of each fetus was determined as previously described (*2.2.5b Fetus Collection and Analysis*).

To extract RNA, frozen whole fetuses (minus bit of tail to determine sex) were pulverized with a mortar and pestle in liquid nitrogen. RNA was extracted from an aliquot of the

pulverized tissue with QIAzol Lysis Reagent (Qiagen) following the manufacturer's protocol. Extracted RNA was DNAse treated followed by cDNA synthesis using the RevertAid First Strand cDNA Synthesis Kit (Thermo Scientific) was via manufacturer instructions. To determine whether or not AR RNA was present in male and female 19-day fetuses, two reactions of PCR amplification were performed using the synthesized cDNA and AR-specific primers (Table 2.6.2). The initial PCR reaction used 1µl of cDNA and the second reaction used 5 µl of the initial PCR product. PCR conditions were 5 minutes at 95°C, followed by 30 cycles of 30 seconds at 95°C, 30 seconds at 56°C, and 30 seconds at 72°C, concluded with 7 minutes at 72°C. Products were visualized on a 2% agarose gel (1X TBE buffer) with SYBR™ Safe DNA gel stain (Invitrogen™) using a ChemiDoc-ItTS2 Imager (Analytik Jena US, Upland, CA).

2.2.8 Statistical Analysis

Chi-square tests were used to determine whether there was a statistically significant difference between the expected and observed frequencies of mutation at different gRNA target loci, the number of AR mutated female and male fetuses, and the number of AR mutated female and male blastocysts. A P-value less than or equal to 0.05 was reported as significant.

2.3 Results

2.3.1 Guide RNA Design and Evaluation in Embryos

Two gRNAs were designed to target exon 2 and one gRNA was designed to target exon 5 of the AR gene in the pig genome (Table 2.6.1, Figure 2.6.1). Zygotes were initially microinjected with Cas9 protein and gRNAs AR_2A, AR_2B, and AR_5 individually before electroporation conditions were established. AR_2A and AR_2B had mutation rates of 100% (3/3 and 4/4 respectively), while AR_5 had a mutation rate of 57% (4/7). Once electroporation conditions were well established, numerous oocyte collections took place to produce zygotes via

IVF. Guides were first electroporated separately, resulting in mutation rates as follows: AR_2A: 12/15 (80%), AR_2B: 8/8 (100%) and AR_5: 9/13 (69%). Guides AR_2A and AR_2B were used in combination and produced 15/18 edited embryos (83%) (Table 2.6.3).

2.3.2 Embryo Transfer Results and Fetus Sequencing

Based on results from testing each gRNA or combination of gRNAs in in vitro produced embryos, all three gRNAs were used during electroporation to mutate AR exons 2 and 5 of embryos that were transferred into recipient females. AR_5 was used by itself to target AR exon 5, while AR_2A and AR_2B were used in combination, as they both targeted AR exon 2. A range of 3 to 6 fetuses were collected from each of 5 fetal harvests 22- to 24-days post embryo transfer. Mutation rates for the fetuses collected after each embryo transfer were 4/5 (80%), 3/3 (100%), 6/6 (100%), 4/4 (100%), and 2/5 (40%) (Table 2.6.4). Of the 275 embryos electroporated with gRNAs targeting AR exons 2 and 5 and transferred into recipient sows, 16 AR-edited fetuses were recovered (6%). Nine fetuses edited at the AR_2A or AR_2B locus were recovered from the 127 transferred embryos targeting AR exon 2 (7%). Seven fetuses edited at the AR_5 locus were recovered from the 148 transferred embryos targeting AR exon 5 (5%).

Sequencing results of edited fetuses revealed mutation types from each gRNA. AR_2A generated 3/6 (50%) small mutations (<15 base pairs) and 3/6 (50%) large mutations (>15 base pairs). AR_2B generated 3/9 (33%) small mutations and 6/9 (66%) large mutations. AR_5 generated 6/7 (86%) small mutations and 1/7 (14%) large mutations (Table 2.6.5). Monoallelic mutations were seen in 2/16 (13%) and biallelic mutations were seen in 14/16 (88%) of the recovered gene-edited fetuses (Table 2.6.5).

Embryos electroporated with gRNAs targeting exon 2 and exon 5 were transferred into embryo transfer recipients to determine if one target locus was more efficient at producing gene

edited fetuses. Four recipients that received electroporated embryos targeting exon 2 and exon 5 resulted in a collection of 22- to 24-day fetuses. Another transfer involved fetuses edited at the exon 5 locus (Table 2.6.4). A chi-squared test was used to determine that there was no significant difference between the number of gene edited fetuses obtained after embryo transfer using embryos electroporated with AR_2A and AR_2B (exon 2) compared to AR_5 (exon 5); however, the data is trending towards a significant difference (P=0.07) (Table 2.6.4).

2.3.3 XY Sequencing of Genetically Modified Fetuses and Blastocysts

All 16 of the AR-edited fetuses collected were female, a sex ratio different from 50:50 (P <0.001; Table 2.6.6a). The unedited fetuses recovered from the same embryo transfers included two males and five females, a sex ratio not different from 50:50 (P=0.26; Table 2.6.6a).

PCR and gel electrophoresis were then used to determine the frequency of female and male AR-edited and control blastocysts. Individual blastocysts that were sexed were generated via IVF and accumulated from numerous oocyte collections. Of the 15 edited blastocysts sexed, 8 were female (XX) and 7 were male (XY). This sex ratio did not differ from 50:50 (P=0.79). Unedited control blastocysts resulted in 6 female (XX) and 1 male (XY). Again, the sex ratio did not differ from 50:50 (P=0.06; Table 2.6.6b).

2.3.4 RNA Expression of AR in 19-Day Fetuses

After extraction of DNA and RNA from unedited, 19-day fetuses, DNA was used to identify 3 female and 3 male samples. cDNA was generated from the female and male samples followed by PCR using a previously tested AR primer (Table 2.6.2). Testis cDNA was used as a control sample and previously confirmed GAPDH primers were used as a control gene for each sample. Figure 2.6.3 shows the presence of AR expression in all female and male samples, as well as the control testis. GAPDH expression was also present in all samples.

2.4 Discussion

Prior to this research, genetically engineered AR knockout mice and naturally occurring AR mutations in humans demonstrated compatibility with organismal wellbeing (Yeh et al., 2002; De Gendt et al., 2004; De Gendt et al., 2005; Notini et al., 2005; Lim et al., 2009; Tsai et al., 2006). In addition, the generation of AR knockout pig blastocysts suggested live AR knockout pigs could be generated using the gRNAs designed and tested; however, this was not the case. Pregnancy could not be maintained to full term, lasting no longer than approximately 28 days. Although it was not anticipated, it is plausible that the gRNAs designed and tested for efficiency in blastocysts are embryonic lethal during fetal development. Androgens play a significant role in the establishment and maintenance of pregnancy. It has become evident that androgens are not only a precursor for the synthesis of estrogen, but they also play a direct role in placental development and function, as well as pregnancy (Parsons and Bouma, 2021). Recent studies using pig models have shown the uterus to be an important steroidogenic organ producing androgens and estrogens in early pregnancy (Franczak and Kotwica, 2008; Franczak and Kotwica, 2010; Wojciechowicz et al., 2013). As proteins require functional receptors to signal a physiological response, a potential cause of pregnancy loss is mutation of the AR gene. Unpublished data from our laboratory suggests the pig placenta is providing a source of androgens to bind to ARs in fetuses (T. Berger, pers. comm.). Placentas from 18-day fetuses demonstrated high gene expression of 17α-hydroxylase, a gene involved in making testosterone, indicating a role during early pregnancy.

MicroRNAs (miRNAs) are endogenous, small non-coding RNAs that have a significant impact on the success of mammalian reproduction. Numerous miRNAs have been detected at different stages of pig embryo development including zygotes to early embryos, peri-

implantation embryos (days 10-20 of pregnancy) and their trophoblasts, and placentas on day 90 of gestation (reviewed by Kaczmarek et al., 2020). Unintended disruption of key miRNAs may lead to loss of pregnancy, as they play significant roles in early embryo development and early pregnancy. Mapping of miRNA in the pig genome is still in the initial stages. U2 spliceosomal RNA, which is involved in processing of miRNAs (Agranat-Tamir, 2014), is known to be located on the X chromosome of the pig in the same region as the AR locus. This is not seen in either the mouse or human, providing another potential reason why disruption of the AR gene in pigs is not be compatible with organismal well-being, unlike what is seen in mice and humans.

To mitigate the potential challenge of lethality, gRNAs were designed to target two different exons in the AR gene, exon 2 and exon 5. Targeting exons 1, 2, or 3 were predicted to disrupt both the classical and non-classical AR signaling pathways, whereas targeting exons 4 through 8 should only disrupt the classical signaling pathway (Trakoolijul et al., 2004). Hence one gRNA was intentionally selected to target the latter group of exons as it was proposed that the latter exons may be less disruptive than eliminating both signaling pathways. Fetuses resulting from embryos electroporated with gRNAs targeting exon 2 and exon 5 were recovered. Statistical analysis showed no significant difference between the two targets; however, results trended towards recovering more exon 2 edited fetuses when they were in potential competition in the same recipient. More embryo transfers should be performed to recover a larger number of samples for a more powerful comparison of exon target sites.

Interestingly, all of the edited fetuses collected 22- to 24-days post embryo transfer were female (XX) ($P<0.001$). To further explore this phenomenon, blastocysts generated via IVF were sequenced and determined to not differ from the expected 50:50 sex ratio. The data suggests

male conceptuses are lost after the blastocyst stage of development in the AR-edited conceptuses while female conceptuses remained until day 24.

AR RNA expression was evaluated in both female and male control 19-day fetuses and AR expression was detected in all female and male 19-day fetuses without an obvious sex difference. Visualizing AR gene expression in 19-day fetuses suggests AR serves a role in early fetal development. Due to AR's location on the X chromosome, a potential explanation for the occurrence of all female fetuses at 24 days is X chromosome inactivation (XCI). For genes located on the X chromosome, full gene expression from both X chromosomes would lead to an imbalance of protein expression and interactions, so cells inactivate or silence one X chromosome (Lyon, 1962). DNA is packaged into a mass by a long noncoding RNA called XIST, which coats the DNA and turns it into silent heterochromatin (Lyon, 2002). However, some genes do not stay silent and are called "escapees", demonstrating varying levels of expression (Carrell and Brown, 2017). With X-linked mutations, females may have compensated expression from the second X chromosome, while mutation of the single X chromosome in males results in lethality (Carrell and Brown, 2017). During this research, the two females with monoallelic edits would have had expression in cells in which the X chromosome containing the edit was inactivated, potentially providing females with monoallelic edits an advantage over males with monoallelic edits. However, the vast majority of edits were biallelic so random X-inactivation does not explain the sex bias.

2.5 Conclusion

Future research should be pursued to determine if designing gRNAs targeting different loci in the AR gene could lead to the generation of live AR knockout pigs. It is plausible that the current gRNA sequences are active at an off-target location that is disrupting a gene or miRNA

essential for embryo development or maintenance of pregnancy, although we have no evidence of off-target responses in these embryos. It would be of interest to determine when during embryo development that AR gene-edited male fetuses are being lost, as well as why female fetuses are being lost prematurely by day 28 of pregnancy. This information could lead to insight to the significance of AR during initial male embryo or fetal development and female fetal development past 28 days of pregnancy.

2.6 Tables and Figures

Table 2.6.1. gRNA Sequences. Sequences were designed and tested in embryos to create indels in exon 2 and exon 5 in the porcine AR gene.

Exon	gRNA Name	Sequence (5'→3')
2	AR_2A	GCACCTCGAAAGGTCTTGGA
2	AR_2B	GCTCTCCGGGTGGCACTCAG
5	AR_5	ATGTGACACTGTCAGCTTCT

Table 2.6.2. PCR Primers Used to Amplify On-Target Sites. Primer name, product size, target locus, sequence, and melting temperature (Tm) from NCBI's Primer Blast for PCR primers targeting indicated locus are provided.

Primer Name	Product Size (bp)	Target Locus	Sequence (5'→3')	Tm (°C)
AR_108F	108	AR RNA	TACCTGTGTGCCAGCAGAAAT	60.6
AR_108R			AGCTCCCAGTGTCATCCCT	62.3
GAPDH_F	104	GAPDH RNA	GGTGAAGGTCGGAGTGAACG	57.9
GAPDH_R			TGAAGGGGTCATTGATGGCG	57.7
AR_610F	610	AR_5 Exon 5	TCAGGGAGAAAGCAGGATACG	56.3
AR_610R			AGGGCAAGAAAGGAACAGACAT	56.6
AR_792F	792	AR_2A and AR_2B Exon 2	ACGCATCGTAGCCTGTTGAA	56.9
AR_792R			TGGACACCGACACTGCCTTA	58.5
AR_1170F	1170	AR_2A and AR_2B Exon 2	CATCCCTCTCTGCTTGCTGAA	57.1
AR_1170R			CTGACTATGTGTGCGGGTTGA	56.7
X_F[a]	446	X Gene	GCACCTCTTTGGTATCTGAGAAAGT	56.7
X_R[a]			ACAACCACCTGGAGAGCCACAAGC	63.5
Y_F[b]	163	SRY Gene	TGAACGCTTTCATTGTGTGGTC	56.1
Y_R[b]			GCCAGTAGTCTCTGTGCCTCCT	60.5

[a]Aasen and Medrano, 1990; [b]Pomp et al., 1995

Table 2.6.3. Blastocyst Mutation Rates. Blastocysts were generated via IVF, microinjected or electroporated with gRNA or a combination of gRNAs and Cas9 protein, collected, and Sanger sequenced. Mutation rates were determined for each gRNA or combination of gRNAs for each technique.

gRNA Target	Microinjection Mutation Rate	Electroporation Mutation Rate
AR_2A	3/3 (100%)	12/15 (80%)
AR_2B	4/4 (100%)	8/8 (100%)
AR_2A + AR_2B	-	15/18 (83%)
AR_5	4/7 (57%)	9/13 (69%)

Table 2.6.4. Embryo Transfer Results. A total of 60 to 100 2- to 4- cell embryos were transferred into the oviduct of each recipient gilt. AR_2A + AR_2B indicates gRNAs AR_2A and AR_2B were electroporated in combination. Fetuses collected 22- to 24- days post embryo transfer were sequenced to determine AR mutation. There is no significant difference between the number of gene edited fetuses obtained after embryo transfer using embryos electroporated with gRNAs targeting exon 2 compared to gRNA targeting exon 5 (P=0.07).

AR gRNA Target	No. Embryos Transferred	No. Fetuses	Sequencing (Mutation rate)	Sexing
AR_2A + AR_2B and AR_5	60 (**30**/**30**)	5	4 AR KO (Exon 2) 1 WT (80%)	5/5 XX
AR_2A + AR_2B and AR_5	70 (**35**/**35**)	3	2 AR KO (Exon 2) 1AR KO (Exon 5) (100%)	3/3 XX
AR_2A + AR_2B and AR_5	64 (32/**10**/**22**)*	6	1 AR KO (Exon 2) 3 AR KO (Exon 5) 0 WT (100%)	6/6 XX
AR_5	66 (**33**/33)*	4	3 AR KO (Exon 5) 0 WT (100%)	4/4 XX
AR_2A + AR_2B and AR_5	100 (**40**/**40**/20)*	4 Fetuses, 1 small piece of tissue	2 AR KO (Exon 2) 3 WT (40%)	5/5 XX
Total	275 (AR-targeted)	23	Exon 2: 9/127 transferred Exon 5: 7/148 transferred	23/23 XX

*Number transferred included embryos electroporated with gRNA/Cas9 for an unrelated gene knockout. Bolded values are AR targeted embryos.

Table 2.6.5. Fetus Mutation Types. Gene-edited fetuses sequenced at each gRNA locus. Edited loci were assessed for mutation size and whether the edit was monoallelic or biallelic. Small mutations were considered insertions or deletions less than 15 base pairs. Large mutations were considered insertions or deletions larger than 15 base pairs. The total mutated loci includes the number of mutated loci evaluated for each gRNA.

gRNA	Small Mutation	Large Mutation	Monoallelic	Biallelic	Total No. Mutated Loci
AR_2A	3	3	0	6	6
AR_2B	3	6	1	8	9
AR_5	6	1	1	6	7

Table 2.6.6a. Fetus Sexing Results. PCR was performed on fetal DNA to determine sex of edited and unedited fetuses retrieved after embryo transfer. All edited fetuses were female, regardless of the location of mutation (P<0.001).

AR Mutation Location	XX	XY
AR_2A + AR_2B	9/9	0/9
AR_5	7/7	0/7
Unedited	5/7	2/7

Table 2.6.6b. Blastocyst Sequencing and Sexing Results. PCR was performed on individual blastocyst DNA to determine sex of edited and unedited blastocysts. Rates were expected to be 50% XX, 50% XY. Of the edited blastocysts, no significant difference was seen (P=0.79) from what was expected. Unedited control blastocyst sexing results were also determined to be not significant from what was expected (P=0.06).

Gene Target	Blastocysts Sequenced	Edited Blastocysts	Edited Blastocyst Sex	WT Blastocyst Sex
AR_2A + AR_2B	10	8/10	4/8 XX 4/8 XY	2/2 XX
AR_5	12	7/12	4/7 XX 3/7 XY	4/5 XX 1/5 XY
Total	22	15/22	8/15 XX 7/15 XY	6/7 XX 1/7 XY

Figure 2.6.1. gRNA Location Map. Exon 2 and Exon 5 of the pig AR gene (NCBI Gene ID: 397582) with gRNA and primer locations. AR_2A is represented in orange, AR_2B is represented in green, and AR_5 is represented in blue. PAM sequences are represented in pink.

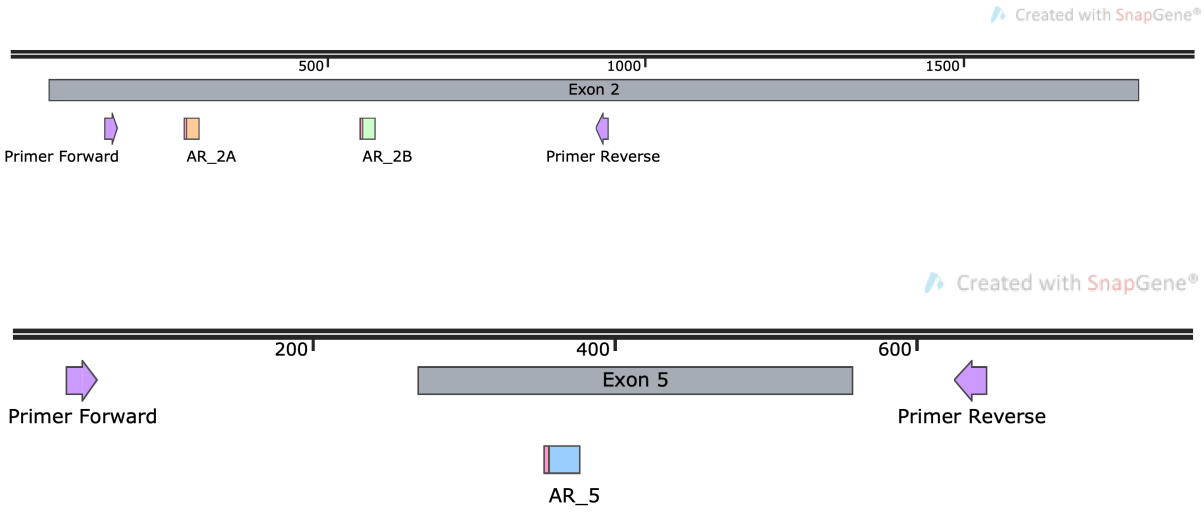

Figure 2.6.2. Fetuses Collected from Embryo Transfers. Fetuses collected 22- to 24- days post embryo transfer. Each row contains fetus and tissue images for one embryo transfer. The upper right-hand corner indicates the gRNA used during electroporation to engineer the genome or **WT** for wild type. The first row pictures one gene-edited fetus electroporated with AR_5 and two gene-edited fetuses electroporated with a combination of AR_2A and AR_2B gRNAs. Row two pictures two gene-edited fetuses electroporated with a combination of AR_2A and AR_2B gRNAs and two unedited fetuses. Row three pictures two gene-edited fetuses electroporated with a combination of AR_2A and AR_2B gRNAs and one unedited fetus.

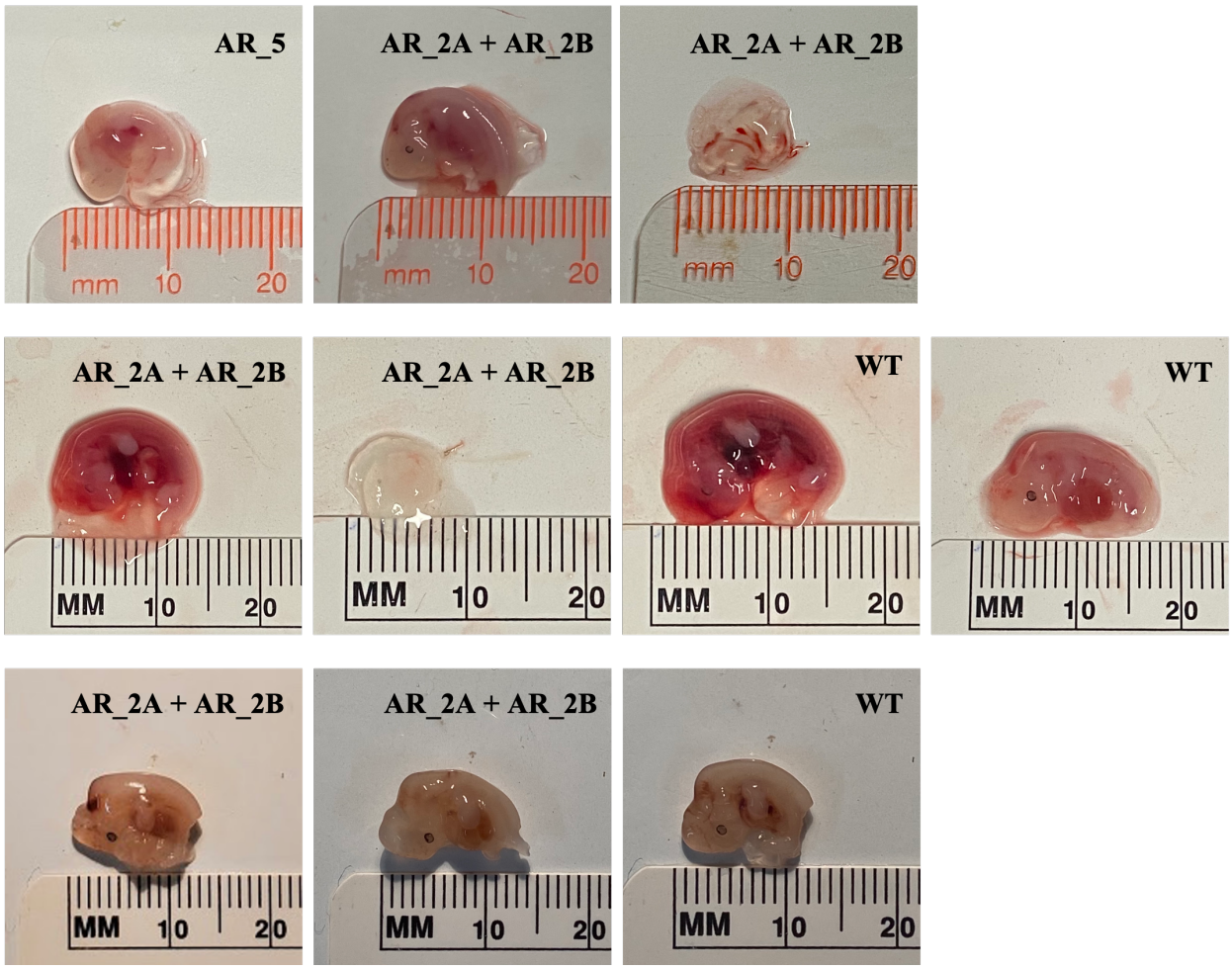

Figure 2.6.3. AR Expression in 19-Day Fetuses. RNA extracted from 19-day female (XX) and male (XY) wild type fetuses was used to detect RNA expression of AR. Boar testis (T) was used as a control. A. 19-day samples showing RNA expression of AR in both female and male samples, as well as control testis. B. 19-day, 26-day, and testis samples showing RNA expression of GAPDH.

A.

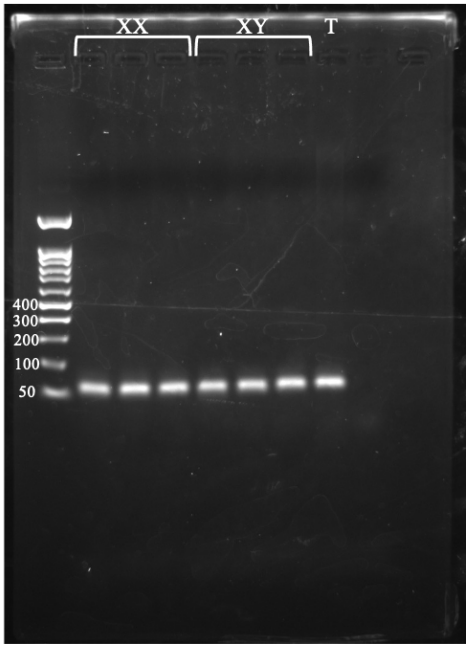

B.

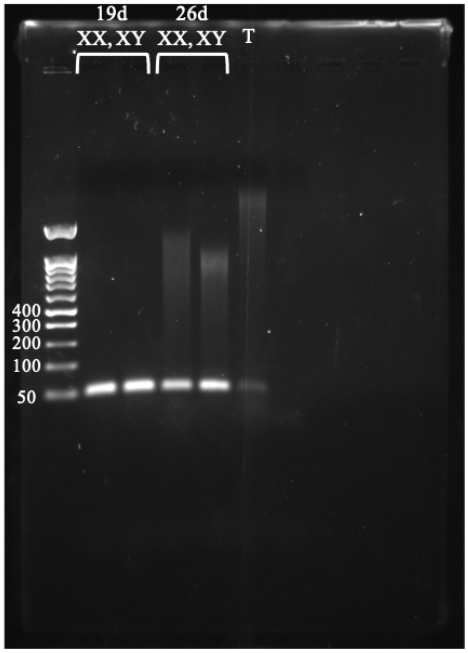

Chapter 3: Off-Target Evaluation of CRISPR Edited Pig Fetuses

3.1 Introduction

3.1.1 CRISPR/Cas9 Off-Target Effects

As with other genetic engineering systems, off-target mutations are a concern when using CRISPR/Cas9 technology. Off-target activity could lead to mutations at unintended sites, potentially resulting in loss of gene function and unintended phenotypes (Naeem et al., 2020). High frequency of off-target activity for RNA-guided endonuclease (RGEN)-induced mutations has been reported; however, reported off-target detection used in silico and in vitro methods, which cannot precisely predict mutations that occur in vivo (Cho et al., 2014, Fu et al., 2013; Zhang et al., 2015). One study assessed off-target activity of various genes in knockout pigs produced via direct injection of CRISPR/Cas9 into embryos and found low prevalence of off-target activity (Carey et al., 2019). For this study, two unrelated genes of interest were selected to generate knockout pig fetuses and evaluate off-target activity. The genes steroid 5 alpha reductase 2 (SRD5A2) and JUNO (folate receptor 4, Folr4) were chosen for off-target analysis while also addressing specific interests relating to pig reproduction.

3.1.2 SRD5A2

Animal welfare concerns surrounding castration are the driving force to develop practical methods to eliminate boar taint, a stale urine and fecal odor and flavor in meat from boars. Castration of male pigs is the current method to remove boar taint; however social pressure has led a push to find alternatives. Some alternatives may include immunocastration, genetic and gender selection, slaughter at a young age, and altering management systems (Lundström and Zamaratskaia, 2006; Valeeva et al., 2009). Immunocastration, or male vaccination against the hormone GnRH, is of concern to pig farmers in terms of food safety, risk to staff administering

vaccinations, economic impacts, and consumer perception (Mancini et al., 2017). Genetic selection for 'low taint' pigs is considered an alternative to reduce boar taint; however, it cannot ensure meat completely void of boar taint and concerns arise as negative effects on growth performance and puberty onset have been seen (Zamaratskaia, 2004; Aldal et al., 2005; Valveeva et al., 2010). While a simple solution, slaughter at a young age is not economically desirable (Mancini et al., 2017). Changes to management systems may reduce the levels of boar taint (Hansen et al., 1994a; Hansen et al., 1994b; Hansen et al., 1997; Van Wagenberg et al., 2013); however, management system changes may not have practical application, as different countries have different regulations (Valeeva et al., 2009). Currently, no dependable alternative to castration exists that guarantees complete elimination of boar taint (Valeeva et al., 2009).

Mistakenly thought to be a product of testosterone, boar taint is primarily caused by the accumulation of compounds androstenone and skatole (Patterson, 1968; Robic et al., 2008). The compounds accumulate in fat and generate offensive odors and flavors, which are perceived by consumers when the meat is heated. Androstenone, an androgen metabolite, is produced in the testis and serves an important reproductive role in male pigs, as it is excreted in saliva and stimulates sexual behavior in females during estrus (Perry et al., 1980). Skatole is a tryptophan metabolite produced by bacterial degradation in the hind gut, where it is absorbed into the blood and deposited into fatty tissues (Squires and Lundström, 1997). Unlike androstenone, skatole is perceived by all consumers (Claus et al., 1994). Androstenone is an ideal target for the elimination of boar taint because it is a main component of boar taint and also inhibits the metabolism of skatole.

The enzyme SRD5A2 synthesizes androstenone from its precursor androstadienone (Robic et al., 2014). By eliminating SRD5A2, the final enzyme required to synthesize

androstenone in the testis, boar taint is both directly and indirectly targeted. Without SRD5A2, androstenone synthesis would no longer occur and skatole metabolism would no longer be inhibited. Thus we hypothesize that boar taint can potentially be eliminated while preserving testosterone, which is necessary for peripubertal growth benefits, increased feed efficiency, and carcass leanness. The long-term goal of this edit is to generate offspring that lack SRD5A2 activity, eliminating androstenone and boar taint in intact males without affecting fertility.

3.1.3 JUNO

Molecular mechanisms behind mammalian fertilization are largely unknown. To achieve successful fertilization, sperm undergo an acrosome reaction, penetrate the zona pellucida, bind to the oocyte's plasma membrane, and finally, fuse with the plasma membrane. Juno and Izumo1 have been identified as the first cell-surface receptor pair essential for fertilization in the mouse (Bianchi et al., 2014). Izumo1 is a protein present under the acrosomal cap of sperm, whose receptor, Juno (folate receptor 4, Folr4) is a protein present on the oocyte plasma membrane.

Izumo1 is present under the plasma membrane and is only exposed and accessible for binding after the acrosome reaction (Inoue et al., 2005). The acrosome reaction, which involves both biochemical and morphological changes of sperm, allows for fertilization to occur by exposing the equatorial segment. After exocytosis of the acrosomal cap, Izumo1 relocates from under the plasma membrane to the equatorial segment of the sperm head (Inoue et al., 2005). To analyze the role of Izumo1 in the fusion of sperm with the oocyte *in vivo*, Izumo-deficient ($Izumo^{-/-}$) mice were generated (Inoue et al., 2005). $Izumo^{-/-}$ females and $Izumo^{+/-}$ males showed normal fertilizing ability. $Izumo^{-/-}$ male mice showed normal mating behavior and ejaculation, however, no pregnancies were observed during a four-month breeding period with wild type females (Inoue et al., 2005). To determine if the defect was limited to sperm-egg fusion or if it

could cause problems in later developmental stages, intracytoplasmic sperm injection (ICSI) was used to bypass the need for sperm-egg fusion. Izumo-deficient sperm injected into the cytoplasm of wild type eggs resulted in fertilized eggs that underwent activation. The fertilized eggs were transplanted into the oviducts of pseudopregnant females and proceeded to implant and develop into heterozygous offspring (Inoue et al., 2005). *In vitro* fertilization (IVF) was used to further explore the sterility of Izumo$^{-/-}$ mice. Izumo1 deficient mice produced sperm capable of undergoing an acrosome reaction, penetrating the ZP, and accumulating in the perivitelline space of the oocytes; however, these sperm were unable to fuse with the oocyte plasma membrane. Overall, the presented information indicates that Izumo1 is required for murine sperm fusion with the oocyte.

The significance of Izumo1 during IVF in pigs was analyzed by Tanihara et al. When anti-IZUMO antisera was added to the fertilization media, fusion of porcine sperm with zona pellucida-free oocytes was slightly but significantly reduced, presumably due to the antisera inhibiting Izumo1 binding with the oocyte plasma membrane (Tanihara et al., 2014). Results from genetic, immunostaining, and *in vitro* experiments, indicate that Izumo1 is essential for sperm-egg fusion, perhaps in multiple species.

Juno was identified as the receptor for Izumo1 on the mouse oocyte (Bianchi et al., 2014). Bianchi and her co-workers demonstrated that (1) Juno is the oocyte surface receptor for Izumo1, (2) the interaction between Izumo1 and Juno is direct, temporary, and the proteins are conserved across mammals, (3) Juno is essential for fertility in female mice, and (4) Juno is rapidly shed from the oolemma of fertilized eggs, suggesting a mechanism to block polyspermy. To show that Juno is essential for murine fertilization, anti-Folr4 antisera was added to the media during IVF and no fertilization was detected (Bianchi et al., 2014). To further explore this

phenomenon, male and female Juno-deficient ($Juno^{-/-}$) mice were developed and bred. After three months of mating, $Juno^{-/-}$ female mice housed with wild type males produced no offspring, showing complete infertility. $Juno^{+/-}$ female mice mated with $Juno^{-/-}$ males demonstrated that heterozygous females were still fertile, as they produced a similar number of offspring as wild type male and female matings. Additionally, $Juno^{-/-}$ oocytes recovered after superovulation were unfertilized though they contained multiple sperm in their perivitelline space, more than oocytes from wild type females. This shows that in vivo, wild type sperm were able to penetrate the zona pellucida; however, the sperm were unable to fuse with the oolemma of $Juno^{-/-}$ oocytes (Bianchi et al., 2014). These findings provide convincing evidence that Izumo1-Juno interaction is necessary for fusion between murine sperm and oocyte.

These experiments have identified Izumo1 and Juno as the first cell-surface receptor pair essential for sperm-egg fusion in mice. However, little work has been done to understand the Izumo1-Juno relationship. In this study, CRISPR/Cas9 technology was used to generate JUNO-deficient pig fetuses to confirm that this is a conserved event across species, as implied by Bianchi et al. 2014.

This study used CRISPR/Cas9 technology to specifically target and mutate SRD5A2 or JUNO to generate knockout fetuses. Candidate guide RNAs (gRNAs) were designed and evaluated for mutation efficiency in pig embryos. Once highly efficient gRNAs were identified, embryos electroporated with Cas9 protein and gRNA were transferred into recipient sows in order to generate and harvest fetuses for analysis. Off-target activity was evaluated by PCR and sequencing of predicted off-target sites for each gRNA.

3.2 Materials and Methods

3.2.1 Animal Care

All experiments were approved and performed in accordance with the Institutional Animal Care and Use Committee (IACUC) at the University of California, Davis. All animals were housed at the UC Davis Swine Facility.

3.2.2 Guide RNA and Primer Design

The Zheng laboratory CRISPR design tool at MIT (crispr.mit.edu) was used to design gRNAs to target exon 1 of SRD5A2 in the *Sus Scrofa* genome. Four gRNAs were identified and selected to avoid off-target events (Table 3.6.1a). For JUNO, gRNAs were designed using Synthego's CRISPR Design Tool (design.synthego.com) to target exon 2 of JUNO in the *Sus Scrofa* genome. One gRNA was chosen based on the software's scoring system, which aims to target an early coding region, be present on a common exon to all transcript variants, combined with high on-target activity, and minimal off target potential (Table 3.6.1b). Once gRNAs were selected for SRD5A2 and JUNO, CRISPRevolution sgRNA EZ Kits (Synthego, Menlo Park, CA) were purchased. Primers were designed using the National Center for Biotechnology Information's primer design software (NCBI's Primer-BLAST (Ye et al., 2012)) to amplify the regions of SRD5A2 (Table 3.6.2a) and JUNO (Table 3.6.2b) flanking each gRNA target site.

3.2.3 Embryo Production

Pig oocytes were collected and matured as previously described in Chapter 2 (*2.2.3a Oocyte Collection and Maturation*). Once matured, oocytes were fertilized via IVF as previously described (*2.2.3b In Vitro Fertilization*).

3.2.4 Guide RNA Evaluation in Embryos

3.2.4a Microinjection and Electroporation

Microinjection and electroporation of pig embryos was performed using the designed gRNA or combination of gRNAs to target SRD5A2 and JUNO, as previously described in Chapter 2 (*2.2.4a Microinjection and Electroporation*).

3.2.4b Embryo Collection and Sequencing

Genomic DNA from embryos electroporated with gRNA or a combination of gRNAs and Cas9 targeting either SRD5A2 or JUNO were sequenced to detect CRISPR/Cas9 induced insertions or deletions (indels). Individual blastocysts were collected as previously described (*2.2.4b Embryo Collection and Sequencing*). Two rounds of PCR were performed using GoTaq Green Master Mix (Promega Biosciences) with specific primers designed to amplify target SRD5A2 (Table 3.6.2a) or JUNO sequences (Table 3.6.2b). The first reaction used 9.2 µl of lysed embryo, while the second reaction used 5 µl of PCR product from the first reaction. The PCR conditions were 5 minutes at 95°C, followed by 35 cycles of 1 minute at 95°C, 1 minute at annealing temperature (Table 3.6.2a and Table 3.6.2b), and 1 minute 30 seconds at 72°C, concluded with 10 minutes at 72°C. PCR products were loaded onto a 0.8% agarose gel (1X TBE buffer) and separated by gel electrophoresis. Bands were extracted using a clean razor blade under UV transillumination. DNA was extracted, purified, and sequenced as previously described in Chapter 2 (*2.2.4b Embryo Collection and Sequencing*). Sequences were aligned to reference SRD5A2 and JUNO sequences using SnapGene® (Insightful Science; available at snapgene.com) and CRISP-ID (Dehairs et al., 2016) software.

3.2.5 Embryo Transfers and Fetus Evaluation

3.2.5a Embryo Transfers

Embryo transfers were performed as previously described in Chapter 2 (*2.2.5a Embryo Transfers*) to obtain fetuses from zygotes generated via IVF and electroporated with gRNA or a

combination of gRNA and Cas9 targeting SRD5A2 or JUNO. For SRD5A2, gRNA targeting exon 1 and exon 2 were used during electroporation and transferred into recipient sows.

3.2.5b Fetus Collection and Analysis

Recipient gilts were slaughtered and fetuses were collected 22- to 24-days post embryo transfer. Tail samples were collected and DNA was extracted, PCR was performed, and products were visualized as previously described in Chapter 2 (*2.2.5b Fetus Collection and Analysis*).

To determine if the collected fetuses contained mutations at the target loci, PCR was performed using GoTaq Green Master Mix (Promega Biosciences) and specific primers designed to amplify the target SRD5A2 and JUNO sequences (Table 3.6.2a and Table 3.6.2b). PCR conditions were previously described (*3.2.4b Embryo Collection and Sequencing*). PCR products were loaded onto a 0.8% agarose gel (1X TBE buffer) and visualized with SYBR™ Safe DNA gel stain (Invitrogen™). Bands of expected and unexpected size were extracted, DNA was purified, samples were submitted for Sanger Sequencing, and sequences were analyzed as previously described (*3.2.4b Embryo Collection and Sequencing*).

3.2.6 Off-Target Analysis of SRD5A2 and JUNO Knockout Blastocysts and Fetuses

3.2.6a Off-Target Site Selection

Software programs CRISPOR (*Nucleic Acids Research*, 2018), CCTop (Stemmer et al., 2015), and CasOffinder (Bae et al., 2014) were used to retrieve and analyze potential off-target sites for each designed SRD5A2 and JUNO gRNA. CRISPOR was used first to obtain a list of potential off-target sites. The sites were listed with the off-target sequence accompanied by a CFD (cutting frequency determination) score and the sequences' genomic position and annotation (exonic, intronic, or intergenic). CCTop and CasOffinder provided similar information for potential off-target sites, including gene name, when applicable.

Off-target site selection for the designed SRD5A2 and JUNO gRNAs was based on CFD score, presence in all three software results, and the site's genomic position and annotation. CFD scores were used to rank the off-target sites for each designed gRNA. Sites with low CFD scores (<0.02) are unlikely to be cleaved, so they were not selected for analysis. Sites located in exonic and intronic regions were considered, while those in intergenic regions were not selected. Five off-target sites that had the highest CFD scores and met the preceding criteria were selected for each designed gRNA. Table 3.6.6a and Table 3.6.6b specify the potential off-target sites for guides SRD_1A, SRD_1B, SRD_2, and JUNO_2, their chromosome, sequence, CFD score, position, and direction.

3.2.6b Off-Target Primer Design and Sequence Validation

Primers were designed to amplify each selected off-target site using the National Center for Biotechnology Information's primer design software (NCBI's Primer-BLAST). For each potential off-target site, porcine genomic DNA from two wild type animals was amplified using the designed primers (Table 3.6.3a and Table 3.6.3b). The PCR conditions were 5 minutes at 95°C, followed by 25 cycles of 45 seconds at 95°C, 45 seconds at annealing temperature (Table 3.6.3a and Table 3.6.3b), and 45 seconds at 72°C, concluded with 7 minutes at 72°C. Products were visualized on a 1% agarose gel (1X TBE buffer) with SYBR™ Safe DNA gel stain (Invitrogen™). Bands were excised using a UV transilluminator and a clean scalpel blade. DNA was extracted and purified using Qiagen's QIAquick Gel Extraction Kit. Samples were submitted to Genewiz (South Plainfield, NJ) for Sanger sequencing. Sequence results were aligned with the anticipated wild type sequences (Ensembl Sscrofa 11.1) using SnapGene® (Insightful Science; available at snapgene.com). Validated wild type animal sequences were later used to compare to knockout fetus sequences.

3.2.6c Off-Target Sequencing of Knockout Fetuses

After verifying the wild type animal sequences matched the anticipated off-target sequences, genomic DNA from confirmed SRD5A2 and JUNO knockout fetuses was amplified using the designed off-target primers for each potential off-target site (Table 3.6.3a and 3.6.3b). PCR conditions were previously described (*3.2.6b Off-Target Primer Design and Sequence Validation*). Products were visualized on a 1% agarose gel (1X TBE buffer) with SYBR™ Safe DNA gel stain (Invitrogen™) and excised using a UV transilluminator and a clean scalpel blade. DNA was extracted, purified, and sequenced as previously described (*3.2.6b Off-Target Primer Design and Sequence Validation*). Sequencing results were aligned with the previously validated wild type sequences using SnapGene®. Gene-edited fetus sequences were compared to wild type to determine if off-target activity had occurred.

3.2.6d Whole Genome Amplification (WGA) and Off-Target Sequencing of SRD5A2 and JUNO Edited Blastocysts

To analyze CRISPR/Cas9 off-target activity in edited SRD5A2 and JUNO blastocysts, whole genome amplification (WGA) was used to amplify DNA from single gene-edited blastocysts. WGA was performed using the remainder of the lysate (5 µl) from previously sequenced SRD5A2 (n=1) and JUNO (n=1) edited blastocysts. Qiagen's REPLI-g® Mini Kit (Cat. No. 150025) was used following manufacturer instructions to complete WGA of the SRD5A2 and JUNO gene-edited samples. GoTaq Green Master Mix, the designed primers for SRD5A2 (Table 3.6.3a, SRD_1A) and JUNO (Table 3.6.3b) off-target sites, and WGA product (1 µl) was used for PCR analysis for each sample. PCR conditions were as previously described (*3.2.6b Off-Target Primer Design and Sequence Validation*). PCR products were run on a 1% agarose gel (1X TBE buffer) and bands were excised using UV transillumination and a clean

scalpel blade. DNA was extracted, purified, and submitted for sequencing as previously described (*3.2.6b Off-Target Primer Design and Sequence Validation*). Off-target sequences from gene-edited blastocysts were compared to wild type sequences using SnapGene® to determine if off-target activity had occurred.

3.2.7 RNA Expression of SRD5A2 in 19- and 26-Day Fetuses

RNA expression of SRD5A2 was evaluated in 19- and 26-day pig fetuses. Wild type females were artificially inseminated with wild type boar semen and 19- and 26-days post-insemination, sows were slaughtered and their fetuses were harvested. All fetuses were collected on dry ice and stored at -80°C. DNA was extracted from a piece of tissue and purified using Qiagen's QIAquick Gel Extraction Kit to determine the sex of each fetus using primers previously confirmed to amplify X and Y regions of porcine DNA (Table 3.6.2a) and PCR conditions previously described (*3.2.5b Fetus Collection and Analysis*). PCR products were visualized on a 2% agarose gel (1X TBE buffer) with SYBR™ Safe DNA gel stain (Invitrogen™) using a ChemiDoc-ItTS2 Imager (Analytik Jena US, Upland, CA) to determine the sex of each fetus.

To extract RNA, whole fetuses (minus a bit of tail to determine sex) were homogenized with a mortar and pestle. Following manufacturer protocol, QIAzol Lysis Reagent (Qiagen) was used to extract RNA from homogenized tissue samples. Extracted RNA was DNAse treated followed by cDNA synthesis. RevertAid First Strand cDNA Synthesis Kit (Thermo Scientific) was used following manufacturer instructions to synthesize cDNA. To determine whether or not SRD5A2 RNA was present in male and female 19- and 26-day fetuses, PCR amplification was performed using the synthesized cDNA and specific SRD5A2 primers (Table 3.6.2a). The initial PCR reaction used 1µl of cDNA and the second reaction used 5 µl of the initial PCR product.

PCR conditions were 5 minutes at 95°C, followed by 30 cycles of 30 seconds at 95°C, 30 seconds at 56°C, and 30 seconds at 72°C, concluded with 7 minutes at 72°C. Products were visualized on a 2% agarose gel (1X TBE buffer) with SYBR™ Safe DNA gel stain (Invitrogen™) using a ChemiDoc-ItTS2 Imager (Analytik Jena US, Upland, CA) to determine the presence or absence of SRD5A2 RNA.

3.3 Results

3.3.1 Guide RNA Design and Evaluation in Embryos

Four gRNA sequences were designed to target SRD5A2 (Table 3.6.1a, Figure 3.6.1a) and one for JUNO (Table 3.6.1b, Figure 3.6.1b) in the pig genome and tested for editing efficiency. Blastocysts generated via IVF were initially microinjected with SRD Guide 1 before electroporation conditions were established. Blastocysts microinjected with SRD Guide 1 and Cas9 protein resulted in 7/11 (64%) edited embryos. Once electroporation conditions were established 1/2 (50%) of blastocysts electroporated with SRD Guide 1 and Cas9 protein were found to be edited. When electroporation conditions were well established, three newly designed gRNAs were tested for editing efficiency. Guides SRD_1A and SRD_1B targeted exon 1 of SRD5A2, while SRD_2 targeted exon 2. Mutation rates were as follows: SRD_1A was 5/6 (83%), SRD_1B was 10/11 (91%), SRD_1A + SRD_1B was 8/8 (100%), and SRD_2 was 6/8 (75%) (Table 3.6.3a). After gRNAs SRD_1A, SRD_1B, and SRD_2 demonstrated higher mutation rates compared to SRD Guide 1, SRD Guide 1 was no longer used for embryo transfers. Due to efficient mutation rates in blastocysts (≥75%), both exon 1 and exon 2 were targeted for mutation during embryo transfers as developmental effects of mutating exon 1 and exon 2 in SRD5A2 fetuses are unknown.

Blastocysts generated via IVF were electroporated with guide JUNO_2 and Cas9 protein to target exon 2 of JUNO in the pig genome resulted in a mutation rate of 19/22 (86%) (Table 3.6.3b). Embryos electroporated with guide JUNO_2 and Cas9 protein were used in embryo transfers.

3.3.2 Embryo Transfer Results and Fetus Sequencing

For SRD5A2, results from testing each gRNA or combination of gRNAs in in vitro produced embryos showed efficient mutation rates, so all three gRNAs were used during embryo transfers. Guides SRD_1A and SRD_1B were used to target SRD5A2 exon 1, while SRD_2 was used to target exon 2. A total of 60 to 100 electroporated embryos were transferred into each of three recipient females, distributed evenly into each oviduct and a range of 3 to 5 fetuses and/or tissues were collected from each fetal harvest 22- to 24-days post embryo transfer. Mutation rates for tissues collected after each embryo transfer were 1/4 (25%), 2/5 (40%), and 3/3 (100%) (Table 3.6.4a). Of the 103 embryos electroporated with gRNAs targeting SRD5A2 and transferred into recipient sows, 4 SRD-edited fetuses were recovered (4%). One fetus edited at the SRD Guide 1 locus was recovered from the 23 transferred embryos targeting SRD5A2 using this SRD Guide 1 (4%). Three fetuses edited at the gRNA SRD_1A locus were recovered from the 20 transferred embryos electroporated with this gRNA (15%). There were no SRD_1B or SRD_2 gene-edited fetuses recovered.

For JUNO, JUNO_2 was electroporated with Cas9 protein in in vitro produced embryos for embryo transfer. A total of 72 to 76 electroporated embryos were transferred into each recipient female, distributed evenly into each oviduct. Two fetal harvests resulted in 2 and 5 fetuses collected. In both collections, 100% of fetuses collected were gene edited. Of the 62

embryos electroporated with gRNA JUNO_2, 5 JUNO-edited fetuses were recovered (8%) (Table 3.6.4b).

Sequencing results of edited fetuses revealed mutation types from each gRNA. SRD Guide 1 generated 1fetus with a large mutation (>15 base pairs). SRD_1A generated 3/3 (100%) small mutations (<15 base pairs). JUNO_2 generated 5/5 (100%) small mutations (Table 3.6.5). Biallelic mutations were seen in all 9 fetuses (100%) (Table 3.6.5).

3.3.3 Off-Target Evaluation in Genetically Modified Fetuses and Blastocysts

Predicted off-target sites for SRD5A2 gRNAs listed in Table 3.6.6a were selected based on the previously specified criteria. Based on the selection criteria, only two potential off-target sites for guide SRD_1A were selected for evaluation. Five predicted off-target sites were selected for guides SRD_1B, SRD_2 and JUNO_2 (Table 3.6.6b). PCR primers were designed to flank each of the selected predicted off-target sites and PCR was carried out using two wild type pig DNA samples with each designed primer pair (Tables 3.6.7a and 3.6.7b) followed by Sanger sequencing and alignment with the predicted sequences reported in Ensembl (Sscrofa 11.1) using SnapGene®. Alignment results showed that each off-target sequence from both wild type animals matched the sequence reported by Ensembl.

After off-target sequence validation using wild type pig DNA, confirmed gene-edited fetuses were evaluated for off-target activity (Table 3.6.8). Off-target site activity was evaluated at off-target sites 1 and 2 for gRNA SRD_1A in the 3 gene-edited conceptuses generated (Table 3.6.6a). Five JUNO gene edited fetuses that were previously collected were evaluated at off-target sites 13, 14, 15, 16, and 17 (Table 3.6.6b). Sequencing results show no off-target activity at any of the seven off-target sites tested in all 8 conceptuses (Table 3.6.8).

To examine potential off-target activity in gene-edited blastocysts, whole genome amplification (WGA) was used to produce enough DNA to complete successful PCR at the off-target loci. One SRD5A2 edited blastocyst and one JUNO edited blastocyst underwent WGA followed by PCR using each designed primer pair (Tables 3.6.7a and 3.6.7b). After sequence alignment with wild type sequences, it was determined DNA from gene-edited blastocysts matched wild type control DNA at all potential off-target sites.

3.3.4 RNA Expression of SRD5A2 in 19- and 26-Day Fetuses

DNA and RNA were extracted from unedited, 19- and 26-day fetuses. DNA was used to identify 2 female and 2 male fetuses from 19- and 26-day groups. cDNA was generated from male and female 19- and 26-day fetuses and Figure 3.6.3 shows the presence of SRD5A2 expression in all female and male samples in 19- and 26-day fetuses, as well as the control testis. GAPDH expression is also seen in all samples.

3.4 Discussion

Although there was success in obtaining knockout 22- to 24-day fetuses for each gene of interest, pregnancies were not maintained. As previously discussed in Chapter 2, there are several potential causes of pregnancy loss including off-target activity and embryonic lethality causing unintended detrimental mutations which would affect embryo development or maintenance of pregnancy. Thus, off-target activity was explored by assessing if any predicted off-target sites were indeed edited in both fetuses and blastocysts.

While multiple, efficient gRNAs could be designed for SRD5A2, there were challenges in obtaining efficient gRNAs for JUNO. Prior to the selection and use of gRNA JUNO_2, numerous other gRNAs were tested for efficiency at generating indels in blastocysts at the JUNO locus; however, the gRNAs showed low mutation efficiency rates (<15%). Some potential

reasons on why numerous gRNAs were unsuccessful at efficiently generating edited blastocysts are the small exon sizes in JUNO, a reduced number of PAM sequences, or an increased number of potential off-target sites. When designing and selecting gRNAs for CRISPR/Cas9, potential off-target sites are important in determining which gRNA or gRNAs should be selected for use. With a smaller exon size, there are less possible gRNA sequences available. If the target exon sequence does not contain many PAM sequences (5'-NGG-3' for *S. Pyogenes*), it lessens the potential number of gRNA sites, as Cas9 requires 5'-NGG-3' to identify, bind, and subsequently cleave the target DNA. Additionally, predicted off-target sites will reduce the number of potential gRNA for a target gene. If there are similar sequences elsewhere in the pig genome, the gRNA will not be identified as a potential option for CRISPR/Cas9. The smaller exon size, which reduces the number of PAM sites, in combination with elimination of gRNA based on predicted off-target sites, decreases the likeliness of designing a highly efficient gRNA for gene editing. The small exon size of JUNO made gRNA design difficult and lead to numerous gRNAs for testing in blastocysts to achieve success with JUNO_2. Future research should perhaps use a dual guide approach. Designing gRNAs flanking exons can be used in combination to delete entire exons. Using this approach would provide more gRNA options.

Although a powerful gene editing tool, CRISPR/Cas9 has the challenge of off-target activity at unintended locations in the genome. A targeted approach to off-target analysis of each SRD5A2 and JUNO gRNA demonstrated no off-target activity at any of the most likely off-target sites predicted by CRISPOR, CCTop, or CasOffinder. This is a significant finding because the two genes of interest are unrelated. Both demonstrated no off-target activity at numerous potential sites that varied in location, CFD score, and position in the pig genome. This was a targeted approach to analyzing off-target activity, as only potential off-targets generated via

software systems were assessed. Only one confirmed knockout for SRD5A2 and one confirmed knockout for JUNO were used to evaluate predicted off-target sites in blastocysts. These results also showed no off-target activity at any of the predicted off-target sites. Increased numbers of confirmed knockout blastocysts for off-target analysis should be used to strengthen these results.

Another potential method to evaluate off-target activity is to use deep sequencing. Recent research used deep sequencing to look at off-target activity for three genes of interest in bovine embryos. Bovine embryos microinjected with gRNA/Cas9 were evaluated for off-target activity at 24 predicted sites using PacBio sequencing (Hennig et al., 2020). There was little to no off-target activity detected. Apart from two targets, no indels were found at the predicted off-target cut sites. Of the two detected targets, neither were detrimental to development, as they were not located in coding or regulatory regions (Hennig et al., 2020). Demonstrating little to no off-target activity in two livestock species at multiple genes of interest indicates off-target activity may not be as large of a concern as previously thought. More studies looking at multiple genes of interest in multiple species is essential to form a clearer picture of off-target activity. Multiple methods to analyze off-target activity would also add to this understanding.

3.5 Conclusion

Evaluating off-target activity in in vivo CRISPR/Cas9 applications is important to determine if off-target activity is a major issue. Further research into true off-target activity levels can lead to improvement of our current genome editing technologies to diminish off-target activity. Generating live SRD5A2 and JUNO knockout pigs is important to further understand the mechanism behind boar taint and its potential as a solution to castration concerns and the biology of fertilization. Further research can help determine why live knockout animals have not been achieved. New gRNAs targeting different loci in each gene may be a solution, as current

gRNA targets may be embryonic lethal. Additionally, using another method to assess off-target activity (e.g. deep sequencing) for the gRNAs being used to modify each gene of interest may also reveal significant unintended off-target modifications.

3.6 Tables and Figures

Table 3.6.1a. gRNA sequences targeting SRD5A2. gRNA sequences designed and tested in embryos to mutate SRD5A2 in the pig genome.

Exon	gRNA	Sequence (5'→3')
1	SRD Guide 1	GAAGCCACTGGCGGGGAATA
1	SRD_1A	CACGGGGTGTCGTTCCATAA
1	SRD_1B	CGCAGGCAAAGGCGCGGATA
2	SRD_2	AAATGTCCTGGGATGCATGG

Table 3.6.1b. gRNA sequences targeting JUNO. gRNA sequence designed and tested in embryos to mutate JUNO in the pig genome.

Exon	gRNA	Sequence (5'→3')
2	JUNO_2	CAGCAGGCATTGTGCTTCCA

Table 3.6.2a. PCR primers used to amplify on-target sites for SRD5A2. Primer name, product size, target locus, sequence, and melting temperature (Tm) are provided.

Primer Name	Product Size (bp)	Target Locus	Sequence (5'→3')	Tm (ºC)
SRD_147F	147	SRD5A2 RNA	ATGGATCGGCTATGCCTTGG	57.4
SRD_147R			AGGGCTTTTCGAGACTTGGG	57.4
GAPDH_F	104	GAPDH RNA	GGTGAAGGTCGGAGTGAACG	57.9
GAPDH_R			TGAAGGGGTCATTGATGGCG	57.7
SRD1AForwSeq	-	Exon 1	GGCCAGGACCTGTATTTGGT	57.3
SRDRevSeq	-	Exon 1	AAAGGGGAAGGACCAAGT	53.4
SRD_693F	693	Exon 1	TGGTTCCATAAAAGCCTTCGTCT	65.0
SRD_693R			GGTCTGCCCGCAATCG	62.0
SRD_877F	877	Exon 1	CGGCTAAATCATCCCTGTGGT	57.2
SRD_877R			GGTCTGCCCGCAATCG	57.0
SRD_1339F	1339	Exon 1	CTGGGGATGAGTATGCGGAG	57.3
SRD_1339R			AGAAAAGGGGTGGTAGGCGA	58.5
SRD_1357F	1357	Exon 1	GCCACCGTGACTCTTTACC	55.7
SRD_1357R			GGAGAAGGAACTGTCTGGGC	57.7
SRD_1759F	1759	Exon 2	TCTGCCTTTTTCGTCTGAGC	55.4
SRD_1759R			CCAAGGAGTTCTGTAGCCCG	57.6
X_F[a]	446	X Gene	GCACCTCTTTGGTATCTGAGAAAGT	56.7
X_R[a]			ACAACCACCTGGAGAGCCACAAGC	63.5
Y_F[b]	163	SRY Gene	TGAACGCTTTCATTGTGTGGTC	56.1
Y_R[b]			GCCAGTAGTCTCTGTGCCTCCT	60.5

[a]Aasen and Medrano, 1990; [b]Pomp et al., 1995

Table 3.6.2b. PCR primers used to amplify on-target sites for JUNO. Primer names, product size, target locus, sequence, and melting temperature (Tm) are provided.

Primer Name	Product Size (bp)	Target Locus	Sequence (5'→3')	Tm (°C)
JunoRevSeq	-	Exon 2	CCAGGCTAGGGGTTCAGTTG	57.7
IZR_700F	700	Exon 2	GGGCAGGGGGAAACATAAGA	57.1
IZR_700R			AATAATCCCTGCATCCCACTGT	56.3
IZR_1302F	1302	Exon 2	CAGGGATGAGGGAGGAGGAA	58.1
IZR_1302R			TGGTTGTCATCGGGGTTGTT	57.0
IZR_1562F	1562	Exon 2	ACGCAAGGTTCACCTCCTCTG	57.4
IZR_1562R			GTCATCGGGGTTGTTGTTCC	56.3
X_F[a]	446	X Gene	GCACCTCTTTGGTATCTGAGAAAGT	56.7
X_R[a]			ACAACCACCTGGAGAGCCACAAGC	63.5
Y_F[b]	163	SRY Gene	TGAACGCTTTCATTGTGTGGTC	56.1
Y_R[b]			GCCAGTAGTCTCTGTGCCTCCT	60.5

[a]Aasen and Medrano, 1990; [b]Pomp et al., 1995

Table 3.6.3a. Blastocyst Mutation Rates for SRD5A2. Blastocysts were generated via IVF, microinjected or electroporated with gRNA or a combination of gRNAs and Cas9 protein, collected, and Sanger sequenced. Mutation rates were determined for each gRNA or combination of gRNAs for each technique.

gRNA Target	Microinjection Mutation Rate	Electroporation Mutation Rate
SRD Guide 1	7/11 (64%)	1/2 (50%)
SRD_1A	-	5/6 (83%)
SRD_1B	-	10/11 (91%)
SRD_1A + SRD_1B	-	8/8 (100%)
SRD_2	-	6/8 (75%)

Table 3.6.3b. Blastocyst Mutation Rates for JUNO. Blastocysts were generated via IVF, electroporated with gRNA JUNO_2 and Cas9 protein to create a mutation at the target locus. After collection of individual blastocysts and Sanger sequencing, mutation rates were determined.

gRNA Target	Electroporation Mutation Rate
JUNO_2	19/22 (86%)

Table 3.6.4a. Embryo Transfer Results for SRD5A2. A total of 60 to 100 2- to 4- cell embryos were transferred into the oviducts of each recipient gilt. Fetuses collected 22- to 24- days post embryo transfer were sequenced to determine SRD5A2 mutation.

gRNA Target	No. Embryos Transferred	Tissues Collected	Sequencing (Mutation rate)	Sexing
SRD Guide 1	69 (**23**/23/23)*	4 Fetuses	1 SRD KO 3 WT (25%)	1/4 XX (WT) 3/4 XY (1 KO, 2 WT)
SRD_1B	100 (40/40/**20**)*	4 Fetuses, 1 Placenta	0 SRD 3 WT (40%)	5/5 XX
SRD_1A, SRD_1B, SRD_2	60 (**20**/**20**/**20**)	2 Fetuses, 1 Placenta	3 SRD_1A KO (100%)	2/3 XX 1/3 XY
Total	103 (SRD-targeted)	12	4/103 transferred	8/12 XX 4/12 XY

* Number transferred included embryos electroporated with gRNA/Cas9 for an unrelated gene knockout. Bolded values are Juno targeted embryos.

Table 3.6.4b. Embryo Transfer Results for JUNO. A total of 72 to 76 2- to 4- cell embryos were transferred into the oviducts of each recipient gilt. Fetuses collected 22- to 24- days post embryo transfer were sequenced to determine JUNO mutation.

gRNA Target	No. Embryos Transferred	No. Fetuses Collected	Sequencing (Mutation rate)	Sexing
JUNO_2	72 (**24**/24/24)*	2	2 JUNO_2 KO (100%)	2/2 XX
JUNO_2	76 (**38**/38)*	5	3 JUNO_2 KO (100%)	5/5 XX
Total	62 (JUNO-targeted)	7	5/62 transferred	7/7 XX

* Number transferred included embryos electroporated with gRNA/Cas9 for an unrelated gene knockout. Bolded values are Juno targeted embryos.

Table 3.6.5. Fetus Mutation Types. Gene-edited fetuses sequenced at each gRNA locus. Edited loci were assessed for mutation size and whether the edit was monoallelic or biallelic. Small mutations were considered insertions or deletions less than 15 base pairs. Large mutations were considered insertions or deletions larger than 15 base pairs. The total mutated loci includes the number of mutated loci evaluated for each gRNA.

gRNA	Small Mutation	Large Mutation	Monoallelic	Biallelic	Total No. Mutated Loci
SRD Guide 1	0	1	0	1	1
SRD_1A	3	0	0	3	3
JUNO_2	5	0	0	5	5

Table 3.6.6a. Predicted off-target sites for three SRD5A2 gRNAs. CRISPOR, CCTop, and CasOffinder were used to retrieve information and select potential off-target sites for analysis. Off-target site number, chromosome location, sequence, CFD score, position, and direction were used for selection. Lowercase bases in off-target sequence indicate mismatch. Five candidates for guide SRD_1B and guide SRD_2 that scored most likely to have off-target activity were chosen for analysis. Only 2 candidates met the selected criteria for guide SRD_1A.

Off-Target Site	Off-Target Chromosome	Off-Target Sequence (5'→3')	CFD Off-Target Score	Position	Direction
SRD_1A					
1	11	CACaGaGTGTCGTcCCATAtTGG	0.15428571444	20877365	+
2	7	gAgaGGGTGTCGTTCCATcACGG	0.0850074963409	3786577	+
SRD_1B					
3	10	aGtAGGCAAAtGCGCGaATAGGG	0.246794871954	59249157	-
4	2	CGCcGGCgctGGCGCGGATACGG	0.13049925817	69117890	+
5	7	CcaAGGCAAAGGCaCGGAgATGG	0.112499999993	121728089	-
6	15	tGCAGaCAAAGGCtCGGATcTGG	0.0606060606091	112778540	+
7	13	tGCAGGCcAAGGCcCGGATcTGG	0.0417439703488	33700074	+
SRD_2					
8	X	gAATGTtCatGGATGCATGGTGG	0.613002232426	3983311	+
9	9	gAATGgCCctGGATGCATGGAGG	0.428571428214	75145358	-
10	9	cAgTGTCtTGGaATGCATGGAGG	0.427777777476	129686468	-

11	15	AAATcTCtgGaGATGCATGGTGG	0.425595238217	126820936	+
12	X	AcATGTCtaGGGAaGCATGGGGG	0.395195578527	86627026	+

Table 3.6.6b. Predicted off-target sites for JUNO_2 gRNA. CRISPOR, CCTop, and CasOffinder were used to retrieve information and select potential off-target sites for analysis. Off-target site number, chromosome location, sequence, CFD score, position, and direction were used for selection. Lowercase bases in off-target sequence indicate mismatch. The 5 candidates most likely to have off-target activity were chosen for analysis.

Off-Target Site	Off-Target Chromosome	Off-Target Sequence (5'→3')	CFD Off-Target Score	Position	Direction
13	8	aAGaAGGCATTGTGCaTCtAAGG	0.353330879898	101235665	+
14	6	aAGgAGGaAaTGTGCTTCCAGGG	0.278571428525	154971534	-
15	3	CAGagGGCAgTGTGCaTCCAGGG	0.275598086045	42650815	-
16	17	gAcaAGGCATTGTGCaTCCACGG	0.268838712889	31911075	+
17	13	CAGaAGtCATaGaGCTTCCAAGG	0.249855407405	31847907	+

Table 3.6.7a. PCR primers used to amplify off-target sites for SRD5A2. Site number, primer names, sequence, and melting temperature (Tm) are provided for PCR primers flanking potential off-target sites for gRNAs SRD_1A, SRD_1B, and SRD_2.

Off-Target Site	Primer Name	Sequences (5'→3')	Tm (°C)
SRD_1A			
1	LRCH1_973F	AGATGGCAGGAGACAGACCT	57.7
	LRCH1_973R	TCAGTTGCCAAGTAGCCGTT	57.0
2	F13A1_694F	TTGTGCCCACTTCTGCTGTA	56.7
	F13A1_694R	ATCTGATGGTGGCTCACGGT	58.7
SRD_1B			
3	CMK1D_756F	CAGCCCTGAGACCTTTCCTC	57.4
	CMK1D_756R	AAAGTTTGCGAGGTCAGGCA	57.5
4	ICAM5_737F	TGAAGGTGCGGAGAGTTGAC	57.2
	ICAM5_737R	GGGTTGCTTCCACATTGCAG	57.2
5	Chrom7_831F	CATTGGCCGGACAAATCGTG	57.1
	Chrom7_831R	GGCTGAGATCGGATGGTGAC	57.7
6	KANSL1L_398F	GGTTAGGGATCTGGCATTGT	54.7
	KANSL1L_398R	CTACTGAGTGTGTGGTGGTATC	54.6
7	DCAF1_858F	GTACGGGGAAGGGAAACAGG	57.7
	DCAF1_858R	GCGGTAGTTTTAAGTGGAACAAA	53.8
SRD_2			
8	X_726F	AATAGATGAGGCGGATGACA	53.3
	X_726R	TGGCTATCCATGCATCTAGC	54.5
9	ASB4_493F	CTCCCGGCAATGACTTACCT	56.9
	ASB4_493R	TCTTGGGGAAGACCGTTGAG	56.8

10	Chrom9_910F	AGGCACCATTGCCTTGTCTT	57.5
	Chrom9_910R	GTCTGGCACAAGGCAGGTAT	57.4
11	Chrom15_997F	TGATGCTCTATTGCAAGTGGT	54.4
	Chrom15_997R	AGAAGACAAAGAAGTAGTTGCCA	54.2
12	NRK_683F	TCAAAATTGCCCAGCAGCATC	56.7
	NRK_683R	GCCAGATTTTATGACCCAAGCC	56.5

Table 3.6.7b. PCR primers to amplify off-target sites for JUNO. Site number, primer names, sequence, and melting temperature (Tm) are provided for PCR primers flanking potential off-target sites for gRNA JUNO_2.

Off-Target Site	Primer	Sequence (5'→3')	Tm (°C)
13	SPATA5_946F	CCACACCAGACCTCAATCCT	56.6
	SPATA5_946R	GCTACACTAGCTGCTCCCTT	56.6
14	DAB1_703F	CAGGAACAGGGCTGAAGGAC	57.9
	DAB1_703R	ACCCTCATACGGATGCTCCA	58.0
15	CARD19_750F	GAGTTCTGGCTCCTCACACC	57.6
	CARD19_750R	CTGGGAGTAGAGCCCTTCCTG	58.9
16	CDC25B_890F	CAGCAAAAAGTGGGGAATGAGG	56.6
	CDC25B_890R	TTCGTTTGGCCCATCTCAGG	57.7
17	C3orf62_995F	GACCAGTCTGTAGCCTAGCAC	57.0
	C3orf62_995R	GCAGGCTCTATGTCCCCAAA	57.3

Table 3.6.8. Off-Target Evaluation in Gene-Edited Fetuses. Off-target sites were evaluated by analysis of sequencing results. Off-target activity was not present at any of the sites in any of the gene-edited fetuses. All sequences aligned with previously confirmed wild type sequences.

Off-Target Site	No. Edited Fetuses Evaluated	Off-Target Activity Rate
SRD_1A		
1	3	0/3
2	3	0/3
JUNO_2		
13	5	0/5
14	5	0/5
15	5	0/5
16	5	0/5
17	5	0/5

Figure 3.6.1a. gRNA Location Map for SRD5A2. Exon 1 and Exon 2 of the pig SRD5A2 gene (NCBI Gene ID: 397048) with gRNA and primer locations. SRD_1A, SRD_1B, SRD Guide 1, and SRD_2 are represented in orange, green, blue, and yellow respectively. PAM locations are in pink.

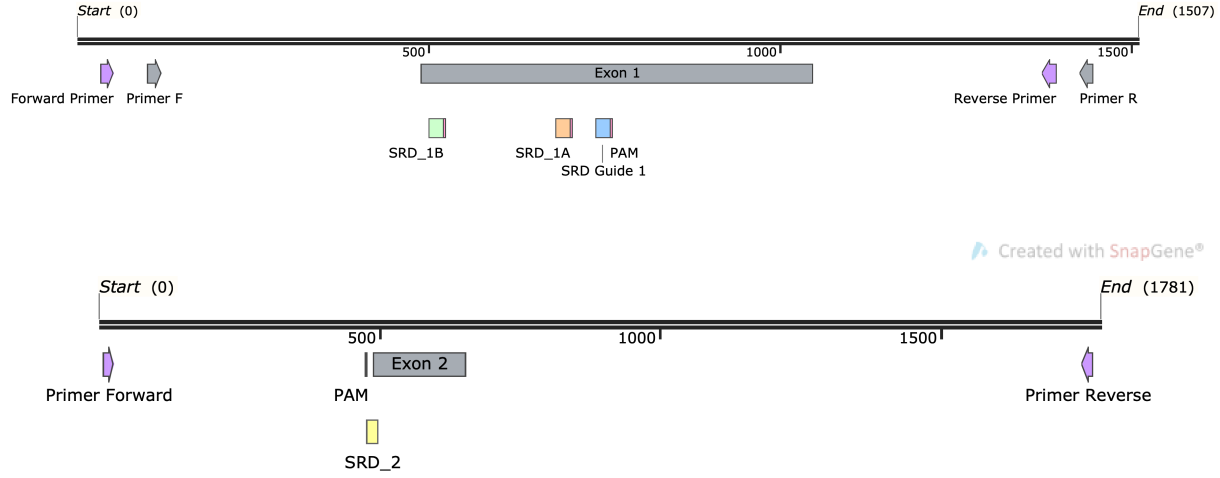

Figure 3.6.1b. gRNA Location Map for JUNO. Exon 2 of the pig JUNO gene (NCBI Gene ID: 102161281) with gRNA and primer locations. JUNO_2 is represented in blue. The PAM sequence is on the left-hand side of JUNO_2 in pink. Primers are also indicated.

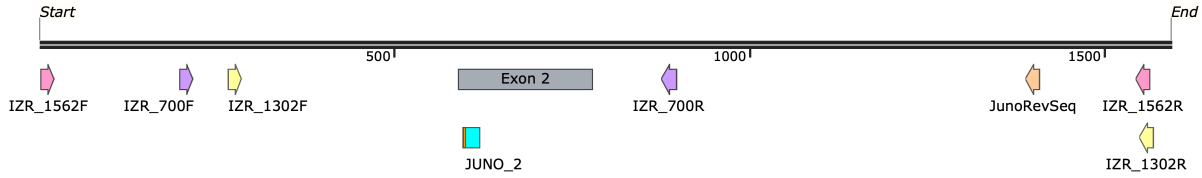

Figure 3.6.2. Fetuses Collected from Embryo Transfers. Fetuses collected 22- to 24-days post embryo transfer. Each row contains fetus and tissue images for an embryo transfer. The upper right-hand corner indicates the gRNA used during electroporation to engineer the genome or **WT** for wild type. **A.** The first row pictures one gene-edited fetus electroporated with SRD Guide 1 and three unedited fetuses. Row two pictures two gene-edited fetuses electroporated with SRD_1A. **B.** Three JUNO-edited samples collected after an embryo transfer are pictured.

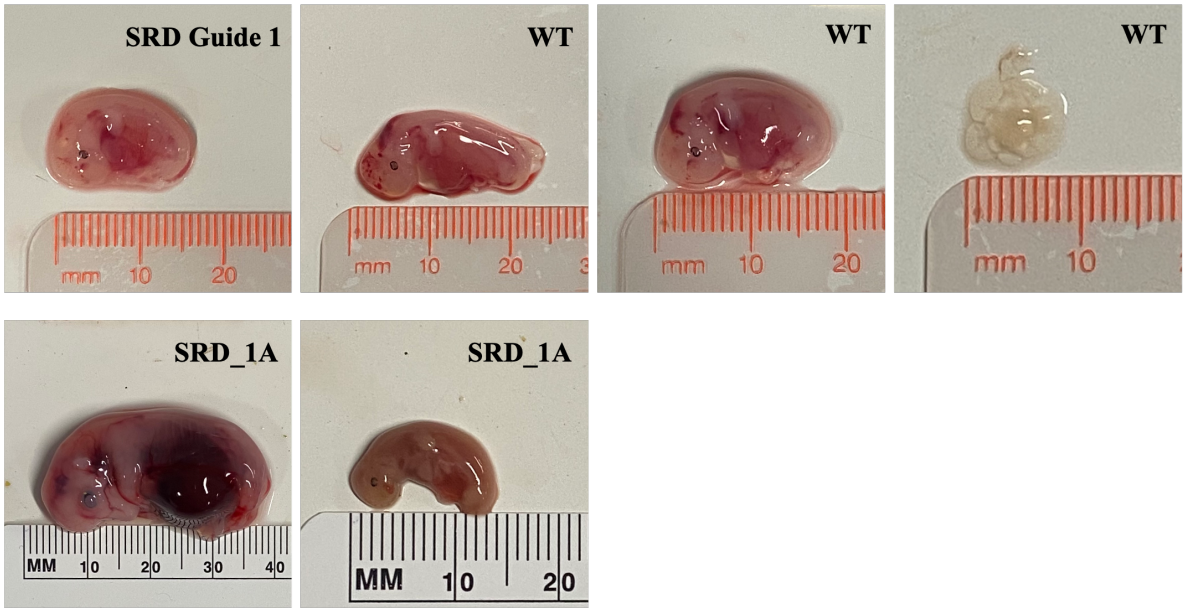

Figure 3.6.3 SRD5A2 Expression in 19- and 26-Day Fetuses. RNA extracted from 19- and 26-day female (XX) and male (XY) wild type fetuses was used to detect RNA expression of SRD5A2. Boar testis (T) was used as a control. A. 19-day samples showing RNA expression of SRD5A2 in both female and male samples, as well as control testis. B. 26-day samples showing RNA expression of SRD5A2 in both female and male samples, as well as control testis. C. 19-day, 26-day, and testis samples showing RNA expression of GAPDH.

A.

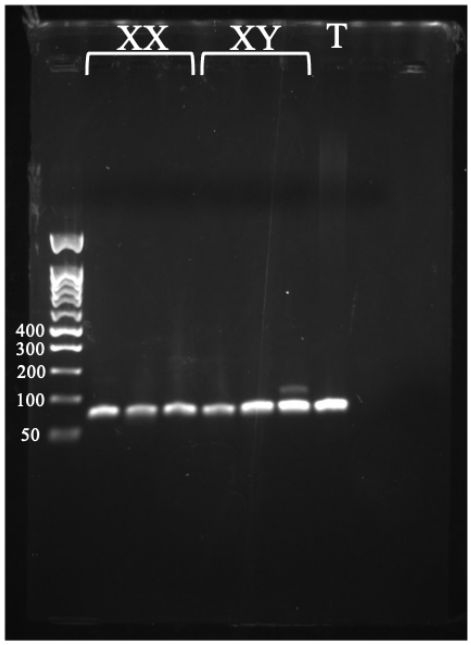

B.

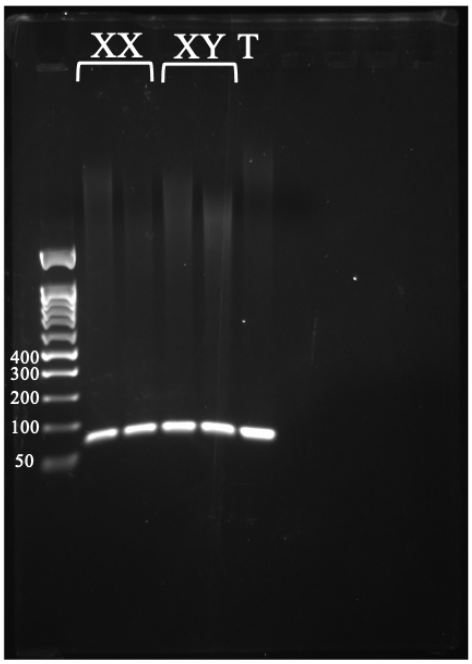

C.

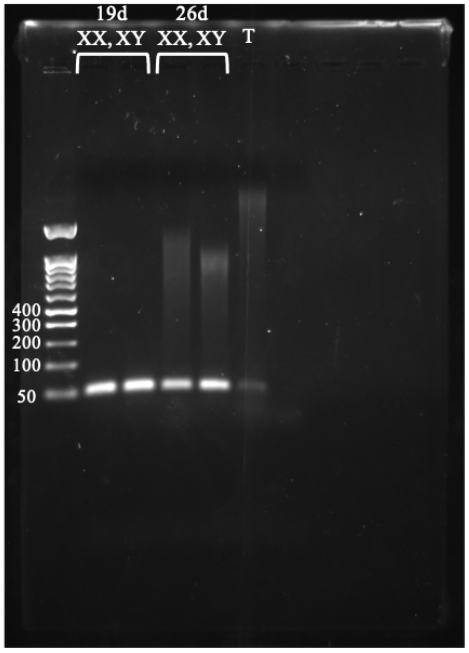

Chapter 4: Summary and Conclusions

The objective of this dissertation research was to utilize CRISPR/Cas9 technology to edit three genes of interest in the pig genome and generate live, knockout animals. Exploring off-target activity was an additional objective, as it is a concern and challenge for researchers working with CRISPR/Cas9. The first gene of interest, androgen receptor (AR) was the focus of Chapter 2. Generating AR knockout pigs has the potential to address containment concerns around genetically modified animals breeding with wild type animals, as well as a point of disruption to eliminate boar taint in intact male pigs. gRNA sequences were designed and tested to modify exons 2 and 5 of the AR gene in the pig genome. They were verified for efficiency in IVF blastocysts and transferred into recipient sows to generate live knockout animals. Although full-term pregnancies were not achieved, 22- to 24-day fetuses were obtained and analyzed. Numerous AR-edited fetuses were generated. It was determined that all AR-edited fetuses were female, different from the expected ratio of 50:50. Although it is still unknown why this event occurred, it is suggested that with AR located on the X chromosome, females compensated with expression from the second X chromosome, while males had an earlier lethality due to a single mutated X chromosome (Carrell and Brown, 2017). For females with monoallelic edits, the presence of AR gene expression from the "inactive" or silent X, potentially allowed female fetuses to survive longer, while males did not survive. However, with the vast majority of fetuses containing biallelic mutations, this does not explain the sex bias. Future research into the timing during embryo development that AR-edited male fetuses did not survive and why female fetuses are being lost prematurely would help determine how to move forward to generate live, gene-edited animals.

The objective of Chapter 3 was to analyze off-target activity in gene-edited fetuses for two unrelated genes of interest. Steroid 5 alpha reductase 2 (SRD5A2) was one gene of interest to address animal welfare concerns surrounding castration to remove boar taint. By eliminating SRD5A2, compounds responsible for boar taint would directly and indirectly be targeted and presumably eliminated. JUNO was the second gene of interest, focusing on the molecular mechanisms behind mammalian fertilization. Juno, an oocyte plasma membrane protein, and Izumo1, a sperm cell surface protein, were identified as the first cell-surface receptor pair essential for fertilization in the mouse (Bianchi et al., 2014). While Juno has been shown to be conserved across multiple species, its function across species has not been confirmed. CRISPR/Cas9 technology followed by embryo transfer and fetal harvest was used to obtain SRD5A2- and JUNO-edited 22- to 24-day fetuses. As with AR, full-term pregnancies were not achieved. There are several theories as to why pregnancies were not maintained for each of the three gene targets. It's plausible for all target genes that the indels are embryonic lethal during fetal development. All three genes of interest play a role in reproduction. AR and SRD5A2 play roles in hormone pathways and JUNO is believed to play a role in fertilization. It is also possible that there is off-target activity affecting genes or miRNAs essential for fetal development or maintenance of pregnancy. miRNAs have a significant impact on the success of mammalian reproduction and there is still a lot unknown. For future research, gRNAs could be redesigned to target new loci within each gene. This could reduce off-target activity or target a less disruptive portion of the gene.

The final objective for this research was to analyze off-target activity in SRD5A2- and JUNO-edited fetuses. Off-target sequencing at every selected predicted off-target site showed no off-target activity in any of the gene-edited fetuses for both SRD5A2 and JUNO gRNAs. A

single edited blastocyst was also evaluated for each gRNA and no off-target activity was detected. More blastocysts could be analyzed to strengthen these results. This was a significant finding as off-target activity is a large concern when working with CRISPR/Cas9. Off-target activity has the potential to lead to mutations at unintended sites, potentially resulting in loss of gene function and unintended phenotypes. High frequency of off-target activity for RNA-guided endonuclease (RGEN)-induced mutations has been reported; however, reported off-target detection used in silico and in vitro methods, which cannot precisely predict mutations that occur in vivo (Cho et al., 2014, Fu et al., 2013; Zhang et al., 2015). Studies assessing off-target activity of human cells found instances where off-target activity was more frequent than the frequency of editing the target sequence (Fu et al., 2013). Other research has shown that using a paired Cas9 nickase system eliminated off-target activity in human cells without reducing on-target efficiency (Cho et al., 2014). Evaluating SRD5A2 and JUNO knockout fetuses not only demonstrated no off-target activity with in vivo derived fetuses but also assessed off-target activity in a livestock species. Off-target research is important to determining if off-target activity is a reasonable concern. Further research can lead to improvement of our current genome engineering techniques to diminish off-target activity and allow for more precise modifications.

The research in this dissertation provides valuable information to move forward with future CRISPR/Cas9 research in pigs. Although live knockout pigs were not obtained, establishing pregnancies to 24 days provides a method for electroporation of pig embryos with CRISPR/Cas9 followed by embryo transfer. Further research to improve the methods provided may lead to reduced potential off-target activity, full-term pregnancies, and live offspring. This would open the door to generating gene-edited pigs that would impact basic science, medicine, biotechnology, and agriculture.

References

Aasen, E., and J. F. Medrano. 1990. Amplification of the Zfy and Zfx genes for sex identification in humans, cattle, sheep and goats. Bio/Technology 8:1279–1281. doi:10.1038/nbt1290-1279.

Adachi, N., H. Suzuki, S. Iiizumi, and H. Koyama. 2003. Hypersensitivity of nonhomologous DNA end-joining mutants to VP-16 and ICRF-193: Implications for the repair of topoisomerase II-mediated DNA damage. J. Biol. Chem. 278:35897–35902. doi:10.1074/JBC.M306500200.

Agranat-Tamir, L., N. Shomron, J. Sperling, and R. Sperling. 2014. Interplay between pre-mRNA splicing and microRNA biogenesis within the supraspliceosome. Nucleic Acids Res. 42:4640–4651. doi:10.1093/NAR/GKT1413.

Ahnesorg, P., P. Smith, and S. P. Jackson. 2006. XLF interacts with the XRCC4-DNA ligase IV complex to promote DNA nonhomologous end-joining. Cell 124:301–313. doi:10.1016/j.cell.2005.12.031.

Aida, T., K. Chiyo, T. Usami, H. Ishikubo, R. Imahashi, Y. Wada, K. F. Tanaka, T. Sakuma, T. Yamamoto, and K. Tanaka. 2015. Cloning-free CRISPR/Cas system facilitates functional cassette knock-in in mice. Genome Biol. 16:1–11. doi:10.1186/S13059-015-0653-X/FIGURES/5.

Aldal, I., Ø. Andresen, A. K. Egeli, J. E. Haugen, A. Grødum, O. Fjetland, and J. L. H. Eikaas. 2005. Levels of androstenone and skatole and the occurrence of boar taint in fat from young boars. Livest. Prod. Sci. 95:121–129. doi:10.1016/j.livprodsci.2004.12.010.

Arnoult, N., A. Correia, J. Ma, A. Merlo, S. Garcia-Gomez, M. Maric, M. Tognetti, C. W. Benner, S. J. Boulton, A. Saghatelian, and J. Karlseder. 2017. Regulation of DNA repair pathway choice in S and G2 phases by the NHEJ inhibitor CYREN. Nature 549:548–552. doi:10.1038/nature24023.

Bae S., J. Park and J.-S. Kim. 2014 Cas-OFFinder: A fast and versatile algorithm that searches for potential off-target sites of Cas9 RNA-guided endonucleases. Bioinformatics 30:1473-1475.

Bailey, S. M., and J. P. Murnane. 2006. Telomeres, chromosome instability and cancer. Nucleic Acids Res 34:2408-2417. doi:10.1093/nar/gkl303.

Barrangou, R., C. Fremaux, H. Deveau, M. Richards, P. Boyaval, S. Moineau, D. A. Romero, and P. Horvath. 2007. CRISPR provides acquired resistance against viruses in prokaryotes. Science. 315:1709–1712. doi:10.1126/science.1138140/suppl_file/barrangou.som.pdf.

Barrangou, R., and P. Horvath. 2012. CRISPR: New horizons in phage resistance and strain identification. Annu. Rev. Food Sci. Technol. 3:143–162. doi:10.1146/ANNUREV-FOOD-022811-101134.

Bertolini, L. R., M. Bertolini, E. A. Maga, K. R. Madden, and J. D. Murray. 2009. Increased gene targeting in Ku70 and Xrcc4 transiently deficient human somatic cells. Mol. Biotechnol. 41:106–114. doi:10.1007/S12033-008-9098-8/TABLES/3.

Bevacqua, R. J., R. Fernandez-Martín, V. Savy, N. G. Canel, M. I. Gismondi, W. A. Kues, D. F. Carlson, S. C. Fahrenkrug, H. Niemann, O. A. Taboga, S. Ferraris, and D. F. Salamone. 2016. Efficient edition of the bovine PRNP prion gene in somatic cells and IVF embryos using the CRISPR/Cas9 system. Theriogenology. 86:1886-1896.e1. doi:10.1016/J.THERIOGENOLOGY.2016.06.010.

Bianchi, E., B. Doe, D. Goulding, and G. J. Wright. 2014. Juno is the egg Izumo receptor and is essential for mammalian fertilization. Nature 508:483-487. doi: 10.1038/nature13203.

Bibikova, M., M. Golic, K. G. Golic, and D. Carroll. 2002. Targeted chromosomal cleavage and mutagenesis in Drosophila using zinc-finger nucleases. Genetics. 161:1169–1175. doi:10.1093/GENETICS/161.3.1169.

Boch, J., and U. Bonas. 2010. Xanthomonas AvrBs3 family-type III effectors: discovery and function. Annu Rev Phytopathol 48:419–436. doi:10.1146/ANNUREV-PHYTO-080508-081936.

Bolotin, A., B. Quinquis, A. Sorokin, and S. Dusko Ehrlich. 2005. Clustered regularly interspaced short palindrome repeats (CRISPRs) have spacers of extrachromosomal origin. Microbiology. 151:2551–2561. doi:10.1099/MIC.0.28048-0.

Brouwer, I., G. Sitters, A. Candelli, S. J. Heerema, I. Heller, A. J. Melo De, H. Zhang, D. Normanno, M. Modesti, E. J. G. Peterman, and G. J. L. Wuite. 2016. Sliding sleeves of XRCC4–XLF bridge DNA and connect fragments of broken DNA. Nature 535:566–569. doi:10.1038/nature18643.

Burger, A., H. Lindsay, A. Felker, C. Hess, C. Anders, E. Chiavacci, J. Zaugg, L. M. Weber, R. Catena, M. Jinek, M. D. Robinson, and C. Mosimann. 2016. Maximizing mutagenesis with solubilized CRISPR-Cas9 ribonucleoprotein complexes. Development. 143:2025–2037. doi:10.1242/DEV.134809.

Carey, K., J. Ryu, K. Uh, A. J. Lengi, S. Clark-Deener, B. A. Corl, and K. Lee. 2019. Frequency of off-targeting in genome edited pigs produced via direct injection of the CRISPR/Cas9 system into developing embryos. BMC Biotechnol. 19:1–8. doi:10.1186/S12896-019-0517-7.

Carrel, L., and C. J. Brown. 2017. When the Lyon(ized chromosome) roars: ongoing expression from an inactive X chromosome. Philos. Trans. R. Soc. Lond. B. Biol. Sci. 372. doi:10.1098/RSTB.2016.0355.

Chance, B., H. Sies, and A. Boveris. 1979. Hydroperoxide metabolism in mammalian organs. Physiol. Rev. 59:527–605. doi:10.1152/PHYSREV.1979.59.3.527.

Chang, H. H. Y., and M. R. Lieber. 2016. Structure-Specific nuclease activities of Artemis and the Artemis: DNA-PKcs complex. Nucleic Acids Res. 44:4991–4997. doi:10.1093/NAR/GKW456.

Chang, H. H. Y., G. Watanabe, and M. R. Lieber. 2015. Unifying the DNA end-processing roles of the artemis nuclease: Ku-dependent artemis resection at blunt DNA ends. J. Biol. Chem. 290:24036–24050. doi:10.1074/JBC.M115.680900.

Chen, Y., X. Liu, Y. Zhang, H. Wang, H. Ying, M. Liu, D. Li, K. O. Lui, and Q. Ding. 2016. A self-restricted CRISPR system to reduce off-target effects. Mol. Ther. 24:1508–1510. doi:10.1038/MT.2016.172.

Cho, S. W., S. Kim, Y. Kim, J. Kweon, H. S. Kim, S. Bae, and J. S. Kim. 2014. Analysis of off-target effects of CRISPR/Cas-derived RNA-guided endonucleases and nickases. Genome Res. 24:132. doi:10.1101/GR.162339.113.

Claus, R., U. Weiler, and A. Herzog. 1994. Physiological aspects of androstenone and skatole formation in the boar-A review with experimental data. Meat Sci. 38:289–305. doi:10.1016/0309-1740(94)90118-X.

Cong, L., F. A. Ran, D. Cox, S. Lin, R. Barretto, N. Habib, P. D. Hsu, X. Wu, W. Jiang, L. A. Marraffini, F. Zhang, M. H. Porteus, D. Baltimore, J. C. Miller, J. D. Sander, A. J. Wood, M. Christian, F. Zhang, J. C. Miller, D. Reyon, et al. 2013. Multiplex genome engineering using CRISPR/Cas systems. Science 339(6121): 819-823. doi:10.1126/science.1231143.

Costantini, F., and E. Lacy. 1981. Introduction of a rabbit β-globin gene into the mouse germ line. Nature 294:92–94. doi:10.1038/294092a0.

Davey, R. A., and M. Grossmann. 2016. Androgen receptor structure, function and biology: from bench to bedside. Clin. Biochem. Rev. 37:3–15.

De Gendt, K., N. Atanassova, K. A. L. Tan, L. R. De França, G. G. Parreira, C. McKinnell, R. M. Sharpe, P. T. K. Saunders, J. I. Mason, S. Hartung, R. Ivell, E. Denolet, and G. Verhoeven. 2005. Development and function of the adult generation of Leydig cells in mice with Sertoli cell-selective or total ablation of the androgen receptor. Endocrinology. 146:4117–4126. doi:10.1210/EN.2005-0300.

De Gendt, K., J. V. Swinnen, P. T. K. Saunders, L. Schoonjans, M. Dewerchin, A. Devos, K. Tan, N. Atanassova, F. Claessens, C. Lécureuil, W. Heyns, P. Carmeliet, F. Guillou, R. M. Sharpe, and G. Verhoeven. 2004. A Sertoli cell-selective knockout of the androgen receptor causes spermatogenic arrest in meiosis. Proc. Natl. Acad. Sci. U. S. A. 101:1327–1332. doi:10.1073/PNAS.0308114100.

Dehairs, J. other authors *et al.* 2016. CRISP-ID: decoding CRISPR mediated indels by Sanger sequencing Sci. Rep. 6:28973; doi: 10.1038/srep28973.

Deltcheva, E., K. Chylinski, C. M. Sharma, K. Gonzales, Y. Chao, Z. A. Pirzada, M. R. Eckert, J. Vogel, and E. Charpentier. 2011. CRISPR RNA maturation by trans-encoded small RNA and host factor RNase III. Nature 471:602-607. doi:10.1038/nature09886.

Doudna, J. A., and E. Charpentier. 2014. Genome editing. The new frontier of genome engineering with CRISPR-Cas9. Science. 346(6213). doi:10.1126/SCIENCE.1258096.

Fu, Y., J. A. Foden, C. Khayter, M. L. Maeder, D. Reyon, J. K. Joung, and J. D. Sander. 2013. High-frequency off-target mutagenesis induced by CRISPR-Cas nucleases in human cells. Nat. Biotechnol. 31:822–826. doi:10.1038/nbt.2623.

Fu, Y., J. D. Sander, D. Reyon, V. M. Cascio, and J. K. Joung. 2014. Improving CRISPR-Cas nuclease specificity using truncated guide RNAs. Nat. Biotechnol.32:279–284. doi:10.1038/nbt.2808.

Franczak, A., and G. Kotwica. 2008. Secretion of estradiol-17beta by porcine endometrium and myometrium during early pregnancy and luteolysis. Theriogenology. 69:283–289. doi:10.1016/J.THERIOGENOLOGY.2007.09.023.

Franczak, A., and G. Kotwica. 2010. Androgens and estradiol-17beta production by porcine uterine cells: In vitro study. Theriogenology. 73:232–241. doi:10.1016/J.THERIOGENOLOGY.2009.09.004.

Gabriel, R., A. Lombardo, A. Arens, J. C. Miller, P. Genovese, C. Kaeppel, A. Nowrouzi, C. C. Bartholomae, J. Wang, G. Friedman, M. C. Holmes, P. D. Gregory, H. Glimm, M. Schmidt, L. Naldini, and C. Von Kalle. 2011. An unbiased genome-wide analysis of zinc-finger nuclease specificity. Nat. Biotechnol. 29:816–823. doi:10.1038/NBT.1948.

Gasiunas, G., R. Barrangou, P. Horvath, and V. Siksnys. 2012. Cas9-crRNA ribonucleoprotein complex mediates specific DNA cleavage for adaptive immunity in bacteria. Proc. Natl. Acad. Sci. U. S. A. 109:E2579–E2586. doi:10.1073/PNAS.1208507109/-/DCSUPPLEMENTAL.

Garas, L.C., J. D. Murray, and E. A. Maga. 2015. Genetically engineered livestock: Ethical use for food and medical models. Ann. Rev. Anim. Biosci. 3:559-575. doi: 10.1146/annurev-animal-022114-110739.

Gordon, J. W., G. A. Scangos, D. J. Plotkin, J. A. Barbosa, and F. H. Ruddle. 1980. Genetic transformation of mouse embryos by microinjection of purified DNA. Proc. Natl. Acad. Sci. USA 77:7380-7384. doi:10.1073/PNAS.77.12.7380.

Gu, J., S. Li, X. Zhang, L.-C. Wang, D. Niewolik, K. Schwarz, R. J. Legerski, E. Zandi, and M. R. Lieber. 2010. DNA-PKcs regulates a single-stranded DNA endonuclease activity of Artemis. DNA Repair (Amst). 9:429. doi:10.1016/J.DNAREP.2010.01.001.

Gupta, R. M., and K. Musunuru. 2014. Expanding the genetic editing tool kit: ZFNs, TALENs, and CRISPR-Cas9. J. Clin. Invest. 124:4154–4161. doi:10.1172/JCI72992.

Hammer, R. E., V. G. Pursel, C. E. Rexroad, R. J. Wall, D. J. Bolt, K. M. Ebert, R. D. Palmiter, and R. L. Brinster. 1985. Production of transgenic rabbits, sheep and pigs by microinjection. Nature 315:680–683. doi:10.1038/315680a0.

Hansen, L. L., A. E. Larsen, B. B. Jensen, and J. Hansen-Møller. 1997. Short time effect of zinc bacitracin and heavy fouling with faeces plus urine on boar taint. Anim. Sci. 64:351–363. doi:10.1017/S1357729800015927.

Hansen, L. L., and A. E. Larsen. 1994a. Effect of antibiotic feed additives on the level of skatole in fat of male pigs. Livest. Prod. Sci. 39:269–274. doi:10.1016/0301-6226(94)90206-2.

Hansen, L. L., A. E. Larsen, B. B. Jensen, J. Hansen-Møller, and P. Barton-Gade. 1994b. Influence of stocking rate and faeces deposition in the pen at different temperatures on skatole concentration (boar taint) in subcutaneous fat. Anim. Prod. 59:99–110. doi:10.1017/S0003356100007546.

Harrison, M. M., B. V. Jenkins, K. M. O'Connor-Giles, and J. Wildonger. 2014. A CRISPR view of development. Genes Dev. 28:1859–1872. doi:10.1101/GAD.248252.114.

Hennig, S. L., J. R. Owen, J. C. Lin, A. E. Young, P. J. Ross, A. L. Van Eenennaam, and J. D. Murray. 2020. Evaluation of mutation rates, mosaicism and off target mutations when injecting Cas9 mRNA or protein for genome editing of bovine embryos. Sci. Reports 10:1–9. doi:10.1038/s41598-020-78264-8.

Horvath, P., and R. Barrangou. 2010. CRISPR/Cas, the immune system of bacteria and archaea. Science. 327:167–170. doi:10.1126/SCIENCE.1179555.

Hsu, P. D., E. S. Lander, and F. Zhang. 2014. Development and applications of CRISPR-Cas9 for genome engineering. Cell. 157:1262–1278. doi:10.1016/J.CELL.2014.05.010.

Ishino, Y., H. Shinagawa, K. Makino, M. Amemura, and A. Nakatura. 1987. Nucleotide sequence of the iap gene, responsible for alkaline phosphatase isozyme conversion in Escherichia coli, and identification of the gene product. J. Bacteriol. 169:5429. doi:10.1128/JB.169.12.5429-5433.1987.

Inoue, N., M. Ikawa, A. Isotani, and M. Okabe. 2005. The immunoglobulin superfamily protein Izumo is required for sperm to fuse with eggs. Nature 434: 234-238. doi: 10.1038/nature03362.

Jao, L. E., S. R. Wente, and W. Chen. 2013. Efficient multiplex biallelic zebrafish genome editing using a CRISPR nuclease system. Proc. Natl. Acad. Sci. U. S. A. 110:13904–13909. doi:10.1073/PNAS.1308335110/-/DCSUPPLEMENTAL.

Jayavaradhan, R., D. M. Pillis, M. Goodman, F. Zhang, Y. Zhang, P. R. Andreassen, and P. Malik. 2019. CRISPR-Cas9 fusion to dominant-negative 53BP1 enhances HDR and inhibits NHEJ specifically at Cas9 target sites. Nat. Commun. 10:1–13. doi:10.1038/s41467-019-10735-7.

Jinek, M., K. Chylinski, I. Fonfara, M. Hauer, J. A. Doudna, and E. Charpentier. 2012. A programmable dual-RNA – guided DNA endonuclease in adaptive bacterial immunity. Science 337:816-821 . doi:10.1126/science.1225829.

Jinek, M., A. East, A. Cheng, S. Lin, E. Ma, and J. Doudna. 2013. RNA-programmed genome editing in human cells. Elife. doi:10.7554/eLife.00471.

Jinek, M., F. Jiang, D. W. Taylor, S. H. Sternberg, E. Kaya, E. Ma, C. Anders, M. Hauer, K. Zhou, S. Lin, M. Kaplan, A. T. Iavarone, E. Charpentier, E. Nogales, and J. A. Doudna. 2014. Structures of Cas9 endonucleases reveal RNA-mediated conformational activation. Science 343(6176):1247997. doi:10.1126/science.1247997.

Kaczmarek, M. M., J. Najmula, M. M. Guzewska, and E. Przygrodzka. 2020. MiRNAs in the peri-implantation period: Contribution to embryo-maternal communication in pigs. Int. J. Mol. Sci. 21. doi:10.3390/IJMS21062229.

Kim, Y., J. Kweon, A. Kim, J. K. Chon, J. Y. Yoo, H. J. Kim, Sojung Kim, C. Lee, E. Jeong, E. Chung, D. Kim, M. S. Lee, E. M. Go, H. J. Song, H. Kim, N. Cho, D. Bang, Seokjoong Kim, and J. S. Kim. 2013. A library of TAL effector nucleases spanning the human genome. Nat. Biotechnol. 31:251–258. doi:10.1038/NBT.2517.

Koike-Yusa, H., Y. Li, E. P. Tan, M. D. C. Velasco-Herrera, and K. Yusa. 2013. Genome-wide recessive genetic screening in mammalian cells with a lentiviral CRISPR-guide RNA library. Nat. Biotechnol. 32:267–273. doi:10.1038/nbt.2800.

Koo, T., J. Lee, and J. S. Kim. 2015. Measuring and reducing off-target activities of programmable nucleases including CRISPR-Cas9. Mol. Cells. 38:475-481. doi:10.14348/molcells.2015.0103.

Lamas-Toranzo, I., B. Galiano-Cogolludo, F. Cornudella-Ardiaca, J. Cobos-Figueroa, O. Ousinde, and P. Bermejo-Álvarez. 2019. Strategies to reduce genetic mosaicism following CRISPR-mediated genome edition in bovine embryos. Sci. Reports 9:1–8. doi:10.1038/s41598-019-51366-8.

Lieber, M. R. 2010. The mechanism of double-strand DNA break repair by the nonhomologous DNA end-joining pathway. Annu. Rev. Biochem. 79:181–211. doi:10.1146/ANNUREV.BIOCHEM.052308.093131.

Lim, P., M. Robson, J. Spaliviero, K. J. McTavish, M. Jimenez, J. D. Zajac, D. J. Handelsman, and C. M. Allan. 2009. Sertoli cell androgen receptor DNA binding domain is essential for the completion of spermatogenesis. Endocrinology. 150:4755–4765. doi:10.1210/EN.2009-0416.

Lundström, K., and G. Zamaratskaia. 2006. Moving towards taint-free pork - Alternatives to surgical castration. In: Acta Veterinaria Scandinavica. Vol. 48. BioMed Central. p. S1.

Lyon, M. F. 2002. X-chromosome inactivation and human genetic disease. Acta Pædiatrica. 91:107–112. doi:10.1111/j.1651-2227.2002.tb03120.x.

Lyon, M. F. 1962. Sex Chromatin and Gene Action in the Mammalian X-Chromosome. Am. J. Hum. Genet. 14:135-148.

MacLean, H. E., G. L. Warne, and J. D. Zajac. 1997. Localization of functional domains in the androgen receptor. J. Steroid Biochem. Mol. Biol. 62:233–242. doi:10.1016/S0960-0760(97)00049-6.

Mak, A. N. S., P. Bradley, A. J. Bogdanove, and B. L. Stoddard. 2013. TAL effectors: function, structure, engineering and applications. Curr. Opin. Struct. Biol. 23:93–99. doi:10.1016/J.SBI.2012.11.001.

Mali, P., J. Aach, P. B. Stranges, K. M. Esvelt, M. Moosburner, S. Kosuri, L. Yang, and G. M. Church. 2013a. CAS9 transcriptional activators for target specificity screening and paired nickases for cooperative genome engineering. Nat. Biotechnol 31:833-838. doi:10.1038/nbt.2675.

Mali, P., L. Yang, K. M. Esvelt, J. Aach, M. Guell, J. E. DiCarlo, J. E. Norville, and G. M. Church. 2013b. RNA-guided human genome engineering via Cas9. Science. doi:10.1126/science.1232033.

Mancini, M. C., D. Menozzi, and F. Arfini. 2017. Immunocastration: Economic implications for the pork supply chain and consumer perception. An assessment of existing research. Livest. Sci. 203:10–20. doi:10.1016/j.livsci.2017.06.012.

Markossian, S., and F. Flamant. 2016. CRISPR/Cas9: a breakthrough in generating mouse models for endocrinologists. J. Mol. Endocrinol. 57:R81–R92. doi:10.1530/JME-15-0305.

Meek, K., V. Dang, and S. P. Lees-Miller. 2008. DNA-PK: the means to justify the ends? Adv. Immunol. 99:33–58. doi:10.1016/S0065-2776(08)00602-0.

Mehravar, M., A. Shirazi, M. Nazari, and M. Banan. 2019. Mosaicism in CRISPR/Cas9-mediated genome editing. Dev. Biol. 445:156–162. doi:10.1016/J.YDBIO.2018.10.008.

Mojica, F. J. M., C. Díez-Villaseñor, E. Soria, and G. Juez. 2000. Biological significance of a family of regularly spaced repeats in the genomes of Archaea, Bacteria and mitochondria. Mol. Microbiol. 36:244–246. doi:10.1046/J.1365-2958.2000.01838.X.

Mojica, F. J. M., C. Díez-Villaseñor, J. García-Martínez, and E. Soria. 2005. Intervening sequences of regularly spaced prokaryotic repeats derive from foreign genetic elements. J. Mol. Evol. 60:174–182. doi:10.1007/S00239-004-0046-3/TABLES/6.

Mussolino, C., R. Morbitzer, F. Lütge, N. Dannemann, T. Lahaye, and T. Cathomen. 2011. A novel TALE nuclease scaffold enables high genome editing activity in combination with low toxicity. Nucleic Acids Res. 39:9283–9293. doi:10.1093/NAR/GKR597.

Naeem, M., S. Majeed, M. Z. Hoque, and I. Ahmad. 2020. Latest developed strategies to minimize the off-target effects in CRISPR-Cas-mediated genome editing. Cells 9(7):1608. doi:10.3390/CELLS9071608.

Nambiar, T. S., P. Billon, G. Diedenhofen, S. B. Hayward, A. Taglialatela, K. Cai, J.-W. Huang, G. Leuzzi, R. Cuella-Martin, A. Palacios, A. Gupta, D. Egli, and A. Ciccia. 2019. Stimulation of CRISPR-mediated homology-directed repair by an engineered RAD18 variant. Nat. Commun. 10:1–13. doi:10.1038/s41467-019-11105-z.

Ni, W., J. Qiao, S. Hu, X. Zhao, M. Regouski, M. Yang, I. A. Polejaeva, and C. Chen. 2014. Efficient gene knockout in goats using CRISPR/Cas9 system. PLoS One. 9:e106718. doi:10.1371/JOURNAL.PONE.0106718.

Nishimasu, H., F. A. Ran, P. D. Hsu, S. Konermann, S. I. Shehata, N. Dohmae, R. Ishitani, F. Zhang, and O. Nureki. 2014. Crystal structure of Cas9 in complex with guide RNA and target DNA. Cell 156(5):935-949. doi:10.1016/j.cell.2014.02.001.

Notini, A. J., R. A. Davey, J. F. McManus, K. L. Bate, and J. D. Zajac. 2005. Genomic actions of the androgen receptor are required for normal male sexual differentiation in a mouse model. J. Mol. Endocrinol. 35:547–555. doi:10.1677/JME.1.01884.

Nucleic Acids Research, Volume 46, Issue W1, 2 July 2018, Pages W242-W245, https://doi.org/10.1093/nar/gky354.

Oliver, D., S. Yuan, H. McSwiggin, and W. Yan. 2015. Pervasive genotypic mosaicism in founder mice derived from genome editing through pronuclear injection. PLoS One 10(6):e0129457. doi:10.1371/JOURNAL.PONE.0129457.

Palmiter, R. D., R. L. Brinster, R. E. Hammer, M. E. Trumbauer, M. G. Rosenfeld, N. C. Birnberg, and R. M. Evans. 1982. Dramatic growth of mice that develop from eggs

microinjected with metallothionein–growth hormone fusion genes. Nature. 300:611–615. doi:10.1038/300611a0.

Pardo, B., B. Gómez-González, and A. Aguilera. 2009. DNA repair in mammalian cells: DNA double-strand break repair: how to fix a broken relationship. Cell. Mol. Life Sci. 66:1039–1056. doi:10.1007/S00018-009-8740-3.

Parsons, A.M. and G. J. Bouma. 2021. A potential role and contribution of androgens in placental development and pregnancy. Life11: 644. https://doi.org/10.3390/life11070644.

Pattanayak, V., C. L. Ramirez, J. K. Joung, and D. R. Liu. 2011. Revealing off-target cleavage specificities of zinc-finger nucleases by in vitro selection. Nat. Methods. 8:765–772. doi:10.1038/NMETH.1670.

Patterson, R. L. S. 1968. 5α-androst-16-ene-3-one:—Compound responsible for taint in boar fat. J. Sci. Food Agric. 19:31–38. doi:10.1002/jsfa.2740190107.

Perry, G. C., R. L. S. Patterson, H. J. H. Macfie, and C. G. Stinson. 1980. Pig courtship behaviour: Pheromonal property of androstene steroids in male submaxillary secretion. Anim. Prod. 31:191–199. doi:10.1017/S0003356100024442.

Pomp, D., B. A. Good, R. D. Geisert, C. J. Corbin, and A. J. Conley. 1995. Sex identification in mammals with polymerase chain reaction and its use to examine sex effects on diameter of day-10 or -11 pig embryos. J. Anim. Sci. 73:1408–1415. doi:10.2527/1995.7351408X.

Pourcel, C., G. Salvignol, and G. Vergnaud. 2005. CRISPR elements in Yersinia pestis acquire new repeats by preferential uptake of bacteriophage DNA, and provide additional tools for evolutionary studies. Microbiology. 151:653–663. doi:10.1099/MIC.0.27437-0.

Ran, F. A., P. D. Hsu, C. Y. Lin, J. S. Gootenberg, S. Konermann, A. E. Trevino, D. A. Scott, A. Inoue, S. Matoba, Y. Zhang, and F. Zhang. 2013. Double nicking by RNA-guided CRISPR cas9 for enhanced genome editing specificity. Cell. 154:1380–1389. doi:10.1016/J.CELL.2013.08.021/ATTACHMENT/04630DBE-53B2-40DA-994A-023E4E4AC5F9/MMC3.PDF.

Raveux, A., S. Vandormael-Pournin, and M. Cohen-Tannoudji. 2017. Optimization of the production of knock-in alleles by CRISPR/Cas9 microinjection into the mouse zygote. Sci. Reports 7:1–11. doi:10.1038/srep42661.

Rees, H. A., W.-H. Yeh, and D. R. Liu. 2019. Development of hRad51–Cas9 nickase fusions that mediate HDR without double-stranded breaks. Nat. Commun. 10:1–12. doi:10.1038/s41467-019-09983-4.

Robic, A., T. Faraut, and A. Prunier. 2014. Pathways and genes involved in steroid hormone metabolism in male pigs: A review and update. J. Steroid Biochem. Mol. Biol. 140:44–55. doi:10.1016/j.jsbmb.2013.11.001.

Robic, A., C. Larzul, and M. Bonneau. 2008. Genetic and metabolic aspects of androstenone and skatole deposition in pig adipose tissue: A review. Genet. Sel. Evol. 40(1):129-143. doi:10.1186/1297-9686-40-1-129.

Ryan, D. E., D. Taussig, I. Steinfeld, S. M. Phadnis, B. D. Lunstad, M. Singh, X. Vuong, K. D. Okochi, R. McCaffrey, M. Olesiak, S. Roy, C. W. Yung, B. Curry, J. R. Sampson, L. Bruhn, and D. J. Dellinger. 2018. Improving CRISPR-Cas specificity with chemical modifications in single-guide RNAs. Nucleic Acids Res. 46:792–803. doi:10.1093/NAR/GKX1199.

Sander, J. D., and J. K. Joung. 2014. CRISPR-Cas systems for editing, regulating and targeting genomes. Nat. Biotechnol. 32:347–355. doi:10.1038/nbt.2842.

Shalem, O., N. E. Sanjana, E. Hartenian, X. Shi, D. A. Scott, T. S. Mikkelsen, D. Heckl, B. L. Ebert, D. E. Root, J. G. Doench, and F. Zhang. 2014. Genome-scale CRISPR-Cas9 knockout screening in human cells. Science. 343:84. doi:10.1126/SCIENCE.1247005.

SnapGene software (from Insightful Science; available at snapgene.com).

Sorek, R., C. M. Lawrence, and B. Wiedenheft. 2013. CRISPR-mediated adaptive immune systems in bacteria and archaea. Annu. Rev. Biochem. 82:237–266. doi:10.1146/ANNUREV-BIOCHEM-072911-172315.

Squires, E. J., and K. Lundström. 1997. Relationship between cytochrome P450IIE1 in liver and levels of skatole and its metabolites in intact male pigs. J. Anim. Sci. 75:2506–2511. doi:10.2527/1997.7592506x.

Stemmer, M., T. Thumberger, M. del Sol Keyer, J. Wittbrodt, and J. L.Mateo. 2015. CCTop: an intuitive, flexible and reliable CRISPR/Cas9 target prediction tool. PLOS ONE 12(4):e0176619. doi: 10.1371/journal.pone.0124633.

Sung, P., L. Krejci, S. Van Komen, and M. G. Sehorn. 2003. Rad51 recombinase and recombination mediators. J. Biol. Chem. 278:42729–42732. doi:10.1074/JBC.R300027200.

Sung, Y. H., J. M. Kim, H.-T. Kim, J. Lee, J. Jeon, Y. Jin, J.-H. Choi, Y. H. Ban, S.-J. Ha, C.-H. Kim, H.-W. Lee, and J.-S. Kim. 2014. Highly efficient gene knockout in mice and zebrafish with RNA-guided endonucleases. Genome Res. 24(1):125-131. doi:10.1101/gr.163394.113.

Tanihara, F., M. Nakai, N. T. h. Men, N. Kato, H. Kaneko, J. Noguchi, T. Otoi, and K. Kikuchi. 2014. Roles of the zona pellucida and functional exposure of the sperm-egg fusion factor “IZUMO” during in vitro fertilization in pigs. Anim. Sci. J. 85:395–404. doi:10.1111/ASJ.12164.

Tanihara, F., M. Hirata, N. T. Nguyen, O. Sawamoto, T. Kikuchi, M. Doi, and T. Otoi. 2020. Efficient generation of GGTA1-deficient pigs by electroporation of the CRISPR/Cas9 system into in vitro-fertilized zygotes. BMC Biotechnol. 20:1–11. doi:10.1186/S12896-020-00638-7/FIGURES/7.

Trakooljul, N., S. Ponsuksili, K. Schellander, and K. Wimmers. 2004. Polymorphisms of the porcine androgen receptor gene affecting its amino acid sequence and expression level. Biochim. Biophys. Acta. 1678:94–101. doi:10.1016/J.BBAEXP.2004.02.004.

Tsai, M. Y., Shauh Der Yeh, R. S. Wang, Shuyuan Yeh, C. Zhang, H. Y. Lin, C. R. Tzeng, and C. Chang. 2006. Differential effects of spermatogenesis and fertility in mice lacking androgen receptor in individual testis cells. Proc. Natl. Acad. Sci. U. S. A. 103:18975–18980. doi:10.1073/PNAS.0608565103.

Urnov, F. D., E. J. Rebar, M. C. Holmes, H. S. Zhang, and P. D. Gregory. 2010. Genome editing with engineered zinc finger nucleases. Nat. Rev. Genet. 11:636–646. doi:10.1038/nrg2842.

Valeeva, N. I., A. de Smet, R. Hoste, and G. B. C. Backus. 2010. Economics of boar taint prevention without surgical castration in the pork chain. Available from: https://www.researchgate.net/publication/46385777_Economics_of_boar_taint_prevention_without_surgical_castration_in_the_pork_chain

Valeeva, N.I., G. B. C. Backus and W. H. M. Baltussen. 2009. Moving towards boar taint-free meat: an overview of alternatives to surgical castration from a chain perspective. Proceedings of the 17th IFMA conference, Bloomington, Illinois, July 19-24, 2009.

van Overbeek, M., D. Capurso, M. M. Carter, M. S. Thompson, E. Frias, C. Russ, J. S. Reece-Hoyes, C. Nye, S. Gradia, B. Vidal, J. Zheng, G. R. Hoffman, C. K. Fuller, and A. P. May. 2016. DNA repair profiling reveals nonrandom outcomes at Cas9-mediated breaks. Mol. Cell. 63:633–646. doi:10.1016/J.MOLCEL.2016.06.037.

Van Wagenberg, C. P. A., H. M. Snoek, J. B. Van Der Fels, C. M. C. Van Der Peet-Schwering, H. M. Vermeer, and L. Heres. 2013. Farm and management characteristics associated with boar taint. Animal. 7:1841–1848. doi:10.1017/S1751731113001328.

Vilarino, M., S. T. Rashid, F. P. Suchy, B. R. McNabb, T. Van Der Meulen, E. J. Fine, S. Ahsan, N. Mursaliyev, V. Sebastiano, S. S. Diab, M. O. Huising, H. Nakauchi, and P. J. Ross. 2017. CRISPR/Cas9 microinjection in oocytes disables pancreas development in sheep. Sci. Reports 7:1–10. doi:10.1038/s41598-017-17805-0.

Wang, Y., X. Cheng, Q. Shan, Y. Zhang, J. Liu, C. Gao, and J. L. Qiu. 2014. Simultaneous editing of three homoeoalleles in hexaploid bread wheat confers heritable resistance to powdery mildew. Nat. Biotechnol. 32:947–951. doi:10.1038/nbt.2969.

Wojciechowicz, B., G. Kotwica, J. Kolakowska, and A. Franczak. 2013. The activity and localization of 3β-hydroxysteroid dehydrogenase/Δ(5)-Δ(4) isomerase and release of androstenedione and progesterone by uterine tissues during early pregnancy and the estrous cycle in pigs. J. Reprod. Dev. 59:49–58. doi:10.1262/JRD.2012-099.

Ye J., G. Coulouris, I. Zaretskaya, I. Cutcutache, S. Rozen, and T. Madden. 2012. Primer-BLAST: A tool to design target-specific primers for polymerase chain reaction. BMC Bioinformatics. 13:134. doi: 10.1186/1471-2105-13-134

Yeh, S., M. Y. Tsai, Q. Xu, X. M. Mu, H. Lardy, K. E. Huang, H. Lin, Shauh Der Yeh, S. Altuwaijri, X. Zhou, L. Xing, B. F. Boyce, M. C. Hung, S. Zhang, L. Gan, and C. Chang. 2002. Generation and characterization of androgen receptor knockout (ARKO) mice: An in vivo model for the study of androgen functions in selective tissues. Proc. Natl. Acad. Sci. U. S. A. 99:13498–13503. doi:10.1073/pnas.212474399.

Yen, S. T., M. Zhang, J. M. Deng, S. J. Usman, C. N. Smith, J. Parker-Thornburg, P. G. Swinton, J. F. Martin, and R. R. Behringer. 2014. Somatic mosaicism and allele complexity induced by CRISPR/Cas9 RNA injections in mouse zygotes. Dev. Biol. 393:3–9. doi:10.1016/J.YDBIO.2014.06.017.

Zamaratskaia, G. 2004. Factors involved in the development of boar taint Influence of breed, age, diet and raising conditions.

Zhang, X. H., L. Y. Tee, X. G. Wang, Q. S. Huang, and S. H. Yang. 2015. Off-target effects in CRISPR/Cas9-mediated genome engineering. Mol. Ther. Nucleic Acids. 4:e264. doi:10.1038/MTNA.2015.37.

Zhao, J., L. Lai, W. Ji, and Q. Zhou. 2019. Genome editing in large animals: current status and future prospects. Natl. Sci. Rev. 6:402-420. doi:10.1093/NSR/NWZ013.

Zickler, D., and N. Kleckner. 1999. Meiotic chromosomes: integrating structure and function. Annu. Rev. Genet. 33:603–754. doi:10.1146/ANNUREV.GENET.33.1.603.